CHALMERS
UNIVERSITY OF TECHNOLOGY

Master's Thesis 2018

Simultaneous S/NO_x control with ClO_2 – Technical Scale Evaluation

Master's thesis in Sustainable Energy Systems

Bengtsson Mathias
Bergqvist Daniel

Department of Space, earth and environment
CHALMERS UNIVERSITY OF TECHNOLOGY
Gothenburg, Sweden 2018

Master's thesis 2018

Master´s Thesis 2018

Simultaneous S/NO_x control with ClO_2 – Technical Scale Evaluation

Bengtsson Mathias
Bergqvist Daniel

CHALMERS
UNIVERSITY OF TECHNOLOGY

Department of Space, earth and environment
Division of Energy Technology
Chalmers University of Technology
Gothenburg, Sweden 2018

Master´s Thesis 2018
Simultaneous S/NO_x control with ClO_2 – Technical Scale Evaluation
Bengtsson Mathias
Bergqvist Daniel

Supervisor: Johansson Jakob, Department of Space, earth and environment
Examiner: Normann Fredrik, Department of Space, earth and environment

Master's Thesis 2018
Department of Space, earth and environment
Division of Energy Technology
Chalmers University of Technology
SE-412 96 Gothenburg
Telephone +46 31 772 1000

Cover: Picture of the scrubber that were used during the technical scale experiments at the Chalmers 100 kW oxy-fuel unit.

Typeset in LaTeX
Printed by Chalmers repro-service
Gothenburg, Sweden 2018

Simultaneous S/NO_x control with ClO_2 - Technical Scale Evaluation
Bengtsson Mathias
Bergqvist Daniel
Department of Space, earth and environment
Chalmers University of Technology

Abstract

Sulfur oxides (SO_x) and nitrogen oxides (NO_x) are major air pollutants that cause acid rain, photochemical smog, and surface ozone accumulation with a number of adverse affects on human health. The removal of SO_x and NO_x from combustion generated flue gases are, therefore, of great importance. Today, the removal of SO_x and NO_x are often made in separate process operations to a considerable cost. This master thesis considers a new concept for simultaneous control of SO_x and NO_x in flue gases through absorption. The concept has previously been tested in lab-scale experiments with promising results and will be evaluated at technical scale in the Chalmers 100kW combustion unit during Year 2018. This master thesis interprets the lab-scale results through a process model to recommend a setup and experimental plan for the technical scale experiments. In addition to this, a discussion on future scale-up to commercial size, of over 10 MW, is also included in this study.

The recommendation for experimental validation is based on simulations made in Aspen Plus where the complete description of the Chalmers 100 kW unit together with detailed chemistry is included. The work concludes that the experimental validation should focus on the pH of the liquid into the scrubber and the liquid to gas ratio over the scrubber, those are the most important process parameters. The recommendation consists of four different cases with large variations in the expected results. To the technical scale experiments that will be performed in the Chalmers 100 kW oxy-fuel unit, a pH of 10 and l/g of 5 to 8 is expected to give the highest removal of both SO_2 and NO_x. The process consists of three main parts, a combustion reactor, a ClO_2-reactor and a scrubber. The scrubber and especially the chemistry inside it, is the main focus of the project.

The results from the simultaneous S/NO_x simulations showed that the removal of SO_x and NO_x in the scrubber will increase with increasing pH in the inlet to the scrubber and a higher liquid to gas ratio. It was concluded that to achieve the highest removal efficiency of NO_x and SO_x in the scrubber, a pH of 10 in the liquid inlet to the scrubber and a liquid to gas ratio of 5 to 8 should be used. The case with pH 10 and 8 l/g with 300 ppm NO_x and 500 ppm SO_2 in the gas inlet to the scrubber resulted in a gas outlet with 21 ppm NO_x and 1 ppm SO_2. A lower l/g in form of 5 will require a lower amount of chemicals and smaller equipment sizes, the gas outlet contained 44 ppm NO_x and 7 ppm SO_2.

Keywords: Flue gas cleaning, Scrubber, Simultaneous, Removal, SO_2, SO_x, NO_x, Aspen Plus.

Acknowledgements

We would like to express our appreciation to the people that have helped us during this master thesis. Our supervisor Jakob Johansson for guiding us through the project. Fredrik Normann our examiner for sharing his knowledge with us. Both of them for giving feedback on our work and the showed interest. Sima Ajdari for helping with Aspen Plus and simplifying the complex chemistry. AkzoNobel for involving us in the development of the simultaneous S/NO_x removal concept. Yara Marine for the information and design of the scrubber unit.

Bengtsson Mathias, Bergqvist Daniel, Gothenburg, June 2018

Contents

List of Figures

List of Tables

1
Introduction

1.1 Background

This master thesis is about control of sulfur oxides (SO_x) and nitrogen oxides (NO_x) emissions from combustion processes. The reasons to control SO_x and NO_x are because they are major air pollutants that can cause acid rain, photochemical smog and ozone accumulation with a number of adverse affects on the human health. Because of the hazardous affects from SO_x and NO_x emissions it is important to have regulations on the maximum amount of SO_x and NO_x that are allowed to be emitted. The european parliament has defined limits of these emissions based on the best available technology (BAT) for each technology, see Table 1.1 for values regarding emission limits for SO_2 and NO_x [1].

Table 1.1: Emission limit values in mg/Nm^3 and *ppm* for SO_2 and NO_x from combustion plants using gaseous fuels. NO_x was approximated as NO_2 when the emission limit value was calculated in *ppm*. The values are calculated at 298 K, at a pressure of 1 atm and at a standardized O_2 content of 3 % [1].

Emitted substance	**Emission limit value** (mg/Nm^3)	**Emission limit value** (*ppm*)
SO_2	35	13
NO_x	100	53

NO_x is formed during combustion in three ways; fuel-, prompt- and thermal NO_x. Depending on combustion conditions, the quantity of formed NO_x from these three mechanisms will differ. SO_x formation depends mainly on sulfur content in fuel. NO_x and SO_x emissions are often controlled in separate units through measures; pre-combustion, during combustion and post-combustion. The main methods that are used to reduce NO_x emissions are during combustion and post-combustion. During combustion usually fuel- and air staging are used. The BAT for post-combustion removal of NO_x is selective catalytic reaction (SCR). Pre-combustion control of SO_x is done by pre-treatment of the fuel to reduce the content of sulfur. SO_x is usually controlled after combustion via wet-scrubbing, so called flue gas desulfurization.

This master thesis is a part of an ongoing project in which Chalmers together with AkzoNobel is developing a process for simultaneous post-combustion control of S/NO_x. This work will develop a process simulation model in Aspen Plus based

on the present understanding of the involved chemistry to be used for planing, evaluating and upscaling a planed pilot scale test campaign. The experimental plan will then be validated during the technical scale experiments of that process in the Chalmers 100 kW oxy-fuel unit. The experimental plan from Aspen Plus will consist of a recommendation of what process parameters to use during the technical scale experiments and four different cases with specific results are also presented.

Previous master thesis has been done by Haunstetter and Weinhart on simultaneous absorption of SO_x and NO_x in cooperation with AkzoNobel Bohus [2]. The thesis included lab-scale experiments on the development of the reaction mechanisms in the oxidation of NO. AkzoNobel has long experience of producing ClO_2 and this could be a new area of use for that chemical. Previous research of the complex liquid phase chemistry between S and N species in the scrubber has been done by Ajdari [3] [4]. The research resulted in a simplification of the chemistry which is used in this thesis, this is further discussed in section 2.5. The scrubber that will be used in the experiments was designed and manufactured by Yara Marine. Yara Marine is already producing scrubbers for marine applications. These scrubbers has earlier only been used to remove SO_x, but due to upcoming law regulations, NO_x control in the scrubber is also of interest. A previous master thesis has been done by Ibrahim on SO_x and NO_x exhaust gas cleaning concept for marine application in cooperation with Yara Marine [5]. That thesis focused mainly on wet-scrubbing for marine removal applications.

1.1.1 Process description

The concept of simultaneous post-combustion control of S/NO_x will be described in this subsection. The concept will be described as the flue gas cleaning section of a combustion process with heat recovery. How the concept could be implemented in a combustion process can be seen in Figure 1.1. The process starts with combustion of a fuel and the formation of flue gases. The flue gases will contain NO, NO_2, SO_2, O_2, CO_2, N_2 and H_2O. More NO will be produced compared to NO_2, because NO is the thermodynamically favored specie from combustion. The energy in the flue gas stream will then be recovered in a heat recovery unit. The flue gases will after that enter the first section of the simultaneous post-combustion control of S/NO_x, an oxidation reactor. The oxidation reactor is used to oxidize NO to NO_2, since NO_2 is more soluble in water. That property can be used to remove NO_2 from the flue gases through scrubbing. An oxidation agent will be used for oxidizing NO to NO_2. The oxidation will occur naturally but is slow without an oxidation agent at standard conditions. After the oxidation, the flue gas will enter in the bottom of a wet-scrubber. Wet-scrubbing is used to remove SO_2 and NO_2 simultaneously by absorbing it into liquid water. During the simultaneous absorption of NO_2 and SO_2 the flue gases will react with the water and form acids that will decrease the pH. Too low pH will effect the reactions, and because of that pH is controlled by addition of a base. The liquid leaving the scrubber will be collected in a process tank, then recycled back into the top of the scrubber after being pH adjusted. A small por-

tion of the liquid stream will be removed from the process for after-treatment and will be handled as a waste stream. The cleaned flue gas will be released from a stack.

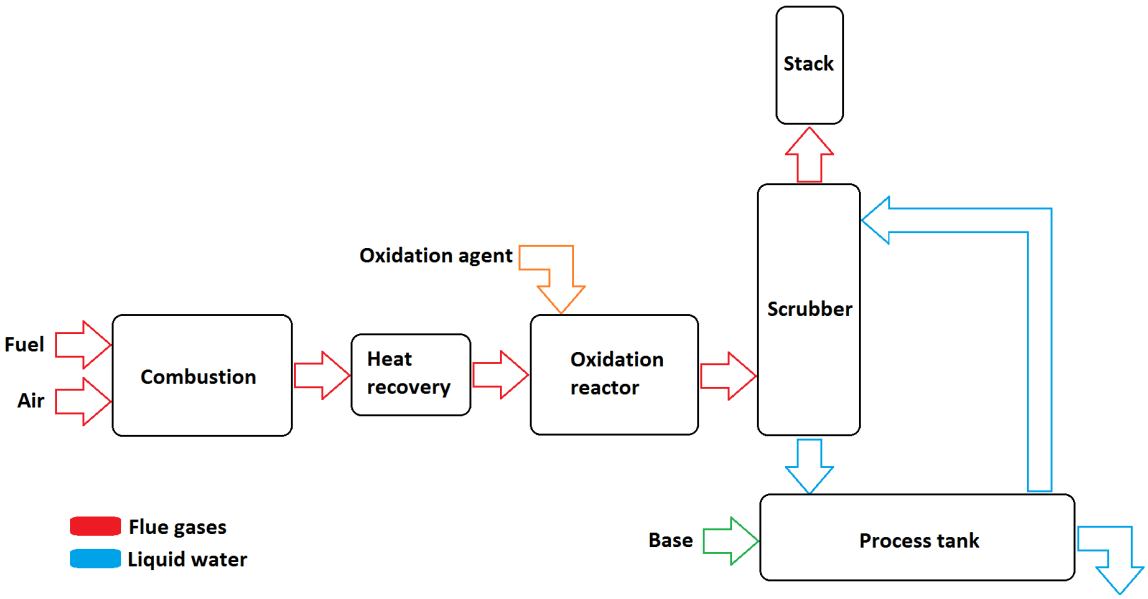

Figure 1.1: The concept of simultaneous post-combustion control of S/NO_x in a combustion process with heat recovery.

1.2 Aim

The overall aim of this thesis is to develop a process simulation model in Aspen Plus based on the present understanding of the involved chemistry to be used for planning and upscaling a planed pilot scale test campaign. Important process parameters will be identified to get valid removal of SO_x and NO_x. Focus is on the scale up from the previously performed lab-scale experiments of about 50 W to technical scale experiments of 80 kW, however scale up to commercial scale of over 10 MW will also be discussed. The work will provide input to design of technical scale experiments at Chalmers 100 kW oxy-fuel unit. The purpose is to make a new contribution to this field of research.

2
Theory

2.1 Formation mechanisms of NO_x and SO_x

During combustion there are three different complex chemical reaction mechanisms that form NO_x. These are; thermal-, fuel- and prompt NO_x formation. Thermal NO_x is the primary source of NO_x formation and is formed from the reaction between oxygen and nitrogen in the combustion air. This formation mechanism is highly dependent on high temperature, the formation peaks between 1900-2000 °C. Fuel NO_x is the formation due to combustion of the organically bound nitrogen in the fuel. This mean that fuel NO_x is dependent on the composition of the fuel that is used for combustion. Gases like propane has lower nitrogen content compared to fossil fuels like oil and coal. The formation of prompt NO_x has the smallest contribution of the three mechanisms. Prompt NO_x is mainly formed in fuel-rich combustion zones. The formation happens when free radicals containing nitrogen (for example HCN, NH and N) reacts quickly with organically bound nitrogen in the fuel [6].

SO_x formation originates mainly from organic and inorganic sulphur compounds in the fuel. During combustion approximately 95 % of the sulphur in the fuel will oxidize to SO_2. SO_x formation is therefore very dependent on the type of fuel [7].

2.2 SO_x and NO_x control

Controlling of SO_x and NO_x emissions can be located at three different stages in the system; pre-combustion, during combustion and post-combustion.

2.2.1 Pre-combustion controls of SO_x

To control the emissions of SO_x the fuel can be shifted to a fuel with lower sulfur content, for example to gases like propane. It could be hard to shift between fuels like propane and coal, due to that different equipment are needed. It is easier to choose the cleaner fuel at design stage. Especially fossil fuels such as coal has a high sulfur content and should not be used if a low amount of SO_x emissions is wanted. If coal necessarily needs to be used, the sulfur can be removed by different pre-combustion control methods [8].

2.2.2 Combustion controls of NO_x

The formation of NO_x can be controlled and reduced by maintaining a lower flame temperature and by using two different methods in form of air- and fuel staging. Air staging reduces the fuel NO_x formation by limiting the available oxygen in the fuel-rich primary zone, due to sub-stoichiometric conditions of air. The lack of oxygen will cause the nitrogen intermediates to form molecular nitrogen instead of NO_x. Secondary air will then be added and the rest of the fuel will be burnt. Staged air intake will have slower fuel-air mixing than a burner without it. Fuel staging is divided into three different zones which are primary-, reburning- and burnout zone. The primary and burnout zone will have excess of air and the reburning zone will have sub-stoichiometric conditions of air. By using this method the peak flame temperature will be reduced resulting in a reduced NO_x formation [6].

The challenge with air- and fuel staging is that they compete with the efficiency of the combustion. Higher flame temperature favors good combustion, but also higher amounts of NO_x. Rapid mixing between fuel and air also ensures good combustion, but will increase the NO_x formation. This mean that these controls need to be balanced to obtain both good combustion efficiency and reduction of NO_x formation [6].

2.2.3 Post-combustion controls of NO_x and SO_x

The most used post-combustion control system to remove NO_x is selective catalytic reduction (SCR). Installed SCR systems are able to reduce 80-90 % of the NO_x emissions. Ammonia is used to reduce NO_x at the surface of a catalyst and produce N_2 and water vapour. Since a catalyst is used, the activation energy is decreased and the reaction can take place at lower temperatures. The temperature range for SCR is 300-450 °C. Above a temperature of 450 °C the ammonia oxides to NO_x and below a temperature of 300 °C the ammonia slip increases. Emissions of ammonia has larger effects on the environment compared to NO_x, which mean that the ammonia slip needs to be kept as low as possible. That is why it is not possible to reach 100 % removal of the NO_x emissions with this technique [6].

Another post-combustion method to reduce NO_x emissions is the selective non catalytic reduction (SNCR). Different types of reagents can be used, the types are;

anhydrous ammonia, aqueous ammonia and urea. The reactions occurs at high temperatures with a peak conversion for the SNCR method at 870-1040 °C. The products that are formed from the reaction are water vapour and molecular nitrogen. If the temperature is above 1040 °C the reaction between ammonia/urea and oxygen will be favoured instead of the reaction with NO. For temperatures below the range the ammonia/urea will be vulnerable for ammonia emissions [6].

SO_x can be removed by different post-combustion methods, example of methods are; scrubbing, adsorption and catalytic oxidation. The scrubbing method is done by spraying a liquid containing a chemical reagent, the liquid absorbs the SO_2 in the flue gas. Usually limestone or magnesium oxide is used as chemical reagent to increase the pH, due to acid formation in the scrubber [9]. The adsorption method is based on activated carbon, sulfur is adsorbed into the activated carbon and oxidized into sulfur trioxide. Washing is used to remove the sulfur trioxide in the form of sulphuric acid. The catalytic method is based on oxidation from sulphur oxide to sulphur trioxide by a catalyst. Sulphuric acid is then formed as in the adsorption method [7].

2.3 Aspen Plus

Aspen Plus is a process simulation and optimization program. Aspen Plus is used in industries and can perform chemical engineering calculations. The program can handle; mass- and energy-balances, mass- and heat-transfer, reactions, etc. In this project the version Aspen Plus V.8.8 is used to simulate the process. Aspen Plus will simulate this process in steady state mode, this is important to remember when comparing the results from Aspen Plus with the results from the technical scale experiments. Due to the fact that during the technical scale experiments steady state might not be reached, because of the long operational time needed. The combustion reactor in the process is modelled as a stoichiometric reactor (RStoic). A plug flow reactor is used to simulate the ClO_2-reactor and two RadFrac towers are used to simulate the scrubber. To be able to change the temperature, add and subtract streams heat exchangers, splitters and mixers are also used.

2.4 Wet scrubber

Wet scrubbing is an industrial technique used to separate certain gases from other gas streams. It operates by introducing the gas streams with a scrubbing liquid, often water. Certain gases are then removed by the scrubbing liquid through absorption. Scrubbers are used as separating method when there are soluble gases present, when the gases cannot be removed easily or safely by dry methods and when a compact separation system is needed. Depending on operating conditions there are many different scrubbers to choose from. The selection depends on gas temperature, gas/gases to be removed, desired efficiency and available space. The

major types of wet scrubbers used in the industry to remove soluble gases are packed towers, tray towers and spray towers [10].

2.5 Technical scale experiments

The concept of simultaneous post-combustion control of S/NO_x described in Subsection 1.1.1 will during 2018 be evaluated in technical scale experiments in the Chalmers 100 kW oxy-fuel unit. An overview of the technical scale experimental setup can be seen in Figure 2.1. This figure can be compared with Figures A.1-A.4 to get a good understanding of how it looks like in real life. There will be some differences between the concept and the technical scale experimental setup, see Figure 1.1 and 2.1. During the technical scale experiments, propane will be used as fuel. Since the fuel not contain sulfur, SO_2 is added in the air inlet. A cooler is used as heat recovery unit. In the experiments ClO_2 will be produced in a ClO_2-generator and ClO_2 will be used as oxidizing agent. The oxidizing of NO to NO_2 will occur in the ClO_2-reactor which is a pipe into the scrubber. The scrubber is a counter current spray column. There are six nozzles that sprays water into the scrubber and the scrubber is divided in two sections. The dimensions of the ClO_2-reactor and the scrubber are stated in Figure 2.1. The diameter of the ClO_2-reactor expands from 0.1 m to 0.2 m. NaOH is used as base during the technical scale experiments.

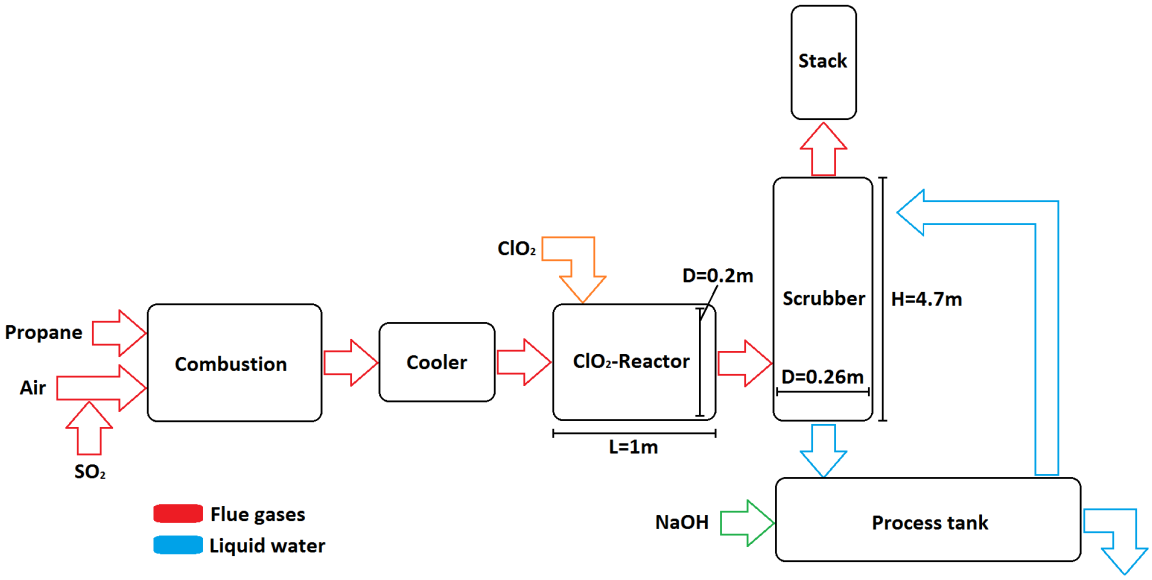

Figure 2.1: An overview of the technical scale experiment setup that will be evaluated in Chalmers 100 kW oxy-fuel.

The most commonly used scrubber is the counter current spray scrubber. In this thesis and also in the technical scale experiments, a counter current spray scrubber will be used to remove NO_2 and SO_2. A sketch of that scrubber can be seen in

Figure 2.2. A picture of the scrubber used during the technical scale experiments can be seen in Figure A.3 and can be compared with the sketch of a counter current spray scrubber. The gas enters in the bottom of the scrubber. The inside of the scrubber is divided in two sections where the liquid is removed between the two sections. The liquid enters at different locations along the scrubber tower. Through nozzles the liquid is sprayed into the scrubber. There are three nozzles in both the top and bottom part of the scrubber. A process tank is integrated with the bottom part of the tower to collect the liquid. To avoid accumulation of liquid in the process a slip stream is used in the reactor tank [10].

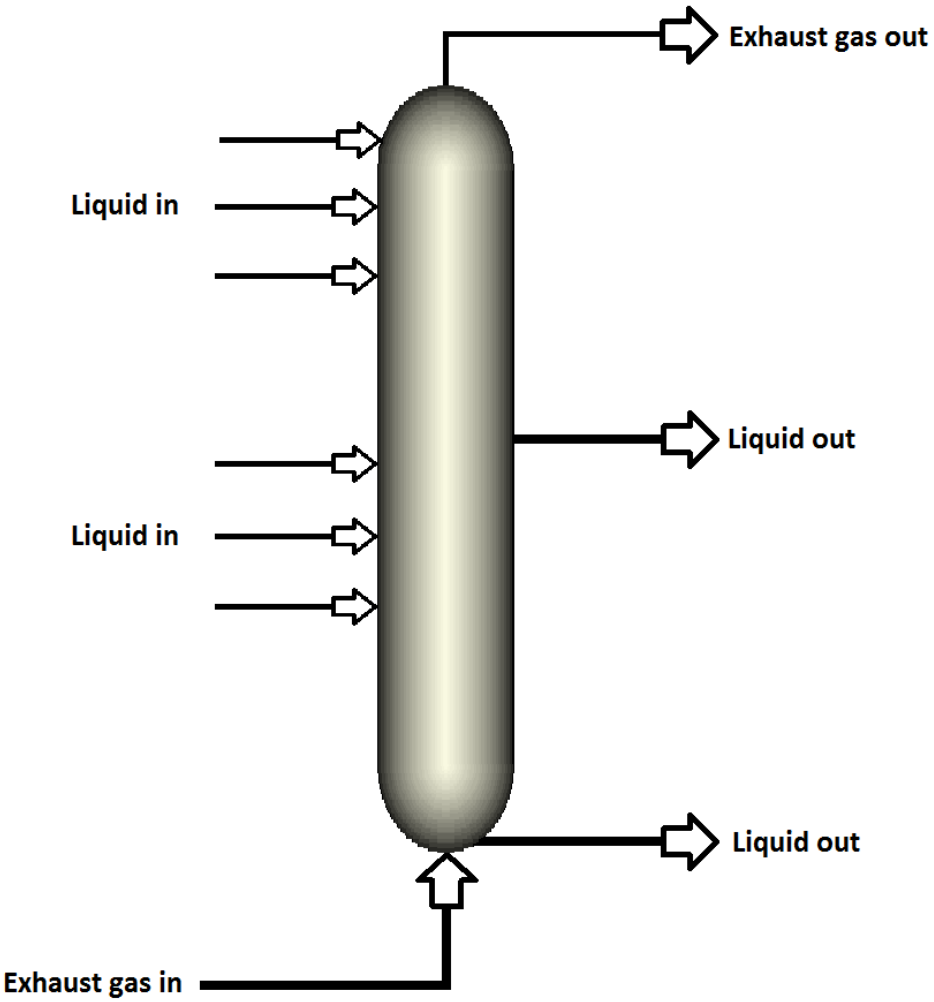

Figure 2.2: Sketch of the counter-current spray scrubber.

2.6 Nitrogen and sulfur chemistry

The chemistry of nitrogen and sulfur species in the liquid phase is complex and not yet fully established. The scrubber simulations are based on the simplified chemistry proposed by Ajdari et. al which is the most comprehensive set to date. The simplified mechanism are shown in Figure 2.3 [3].

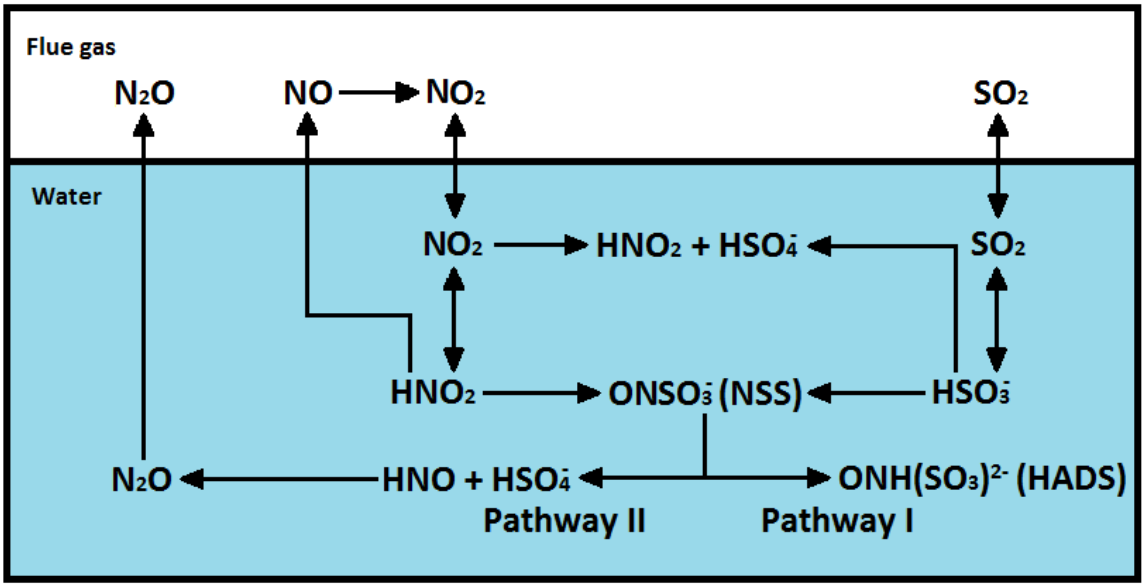

Figure 2.3: Reaction diagram describing the sulfur and nitrogen chemistry in the scrubber when the flue gas gets in contact with the liquid water. This is an updated version of a reaction diagram done by Ajdari et al. [3].

The reaction diagram in Figure 2.3 contains both reactions that are general and valid for all pH conditions and reactions that only occur at specific pH. The flue gas going into the scrubber will contain NO_x and SO_2. Due to the oxidation of NO in the ClO_2-reactor the NO_x will consist of mainly NO_2 and only low amounts of NO. In the gas phase NO will continue to oxidize to NO_2 by reaction with O_2, but this reaction is slow at atmospheric pressure. NO_2 has a relatively high solubility in water (especially compared to NO) and will be absorbed by the liquid water in the scrubber. SO_2 also has high solubility and will quickly be absorbed by the liquid water. Both NO_2 and SO_2 will react with the water and form nitrous acid (HNO_2) and sulfurous acid (HSO_3^-).

The interactions between nitrogen and sulfur in the liquid phase is the above mentioned complex chemistry and has in this thesis been simplified into two types of interactions. The interactions between NO_2 and $S(IV)$ and HNO_2 with HSO_3^-. NO_2 will react with $S(IV)$ and water at pH ≥ 5 and will produce nitrous acid and sulfuric acid (HSO_4^-), according to Reaction (2.1).

$$\text{pH} \geq 5 \qquad NO_2(aq) + HSO_3^-(aq) + H_2O(l) \rightarrow 2HNO_2(aq) + HSO_4^-(aq) \qquad (2.1)$$

The reaction between HNO_2 and HSO_3^- will produce nitrososulfonic acid ($ONSO_3^-$ also known as NSS). Further reaction of NSS depends on the pH of the system, either react according to pathway I or pathway II in Figure 2.3. At pH ≥ 4 pathway I will dominate and NSS will react with HSO_3^- and form hydroxylamine disulfonic acid (HADS) and other similar N-S complexes, according to Reaction (2.2). Reaction (2.2) shows the overall reaction of pathway I, from HNO_2 and HSO_3^- to HADS.

$$\text{pH} \geq 4 \qquad HNO_2(aq) + 2HSO_3^-(aq) \rightarrow HADS(aq) + H_2O(l) \qquad (2.2)$$

At pH ≤ 1 pathway II will dominate and NSS will be hydrolyzed and form N_2O and HSO_4^-, according to Reaction (2.3). Reaction (2.3) shows the overall reaction of pathway II, from HNO_2 and HSO_3^- to N_2O and HSO_4^-.

$$\text{pH} \leq 1 \qquad HNO_2(aq) + 2HSO_3^-(aq) \rightarrow 0.5N_2O(aq) + HSO_4^-(aq) + 0.5H_2O(l) \qquad (2.3)$$

N_2O will then dissolve from the liquid phase into the gas phase. For the pH interval 1-4, pathway I and II will equally dominate. A more advanced reaction diagram describing pathway I and II can be seen in Figure 2.4 compared to Figure 2.3. In Figure 2.4 is HAMS, ATS and ADS the shortening of hydroxylamine monosulfonic acid, amine trisulfonic acid and amine disulfonic acid. When simulating the scrubber in Aspen Plus the simplified reaction diagram in Figure 2.3 will be used [3].

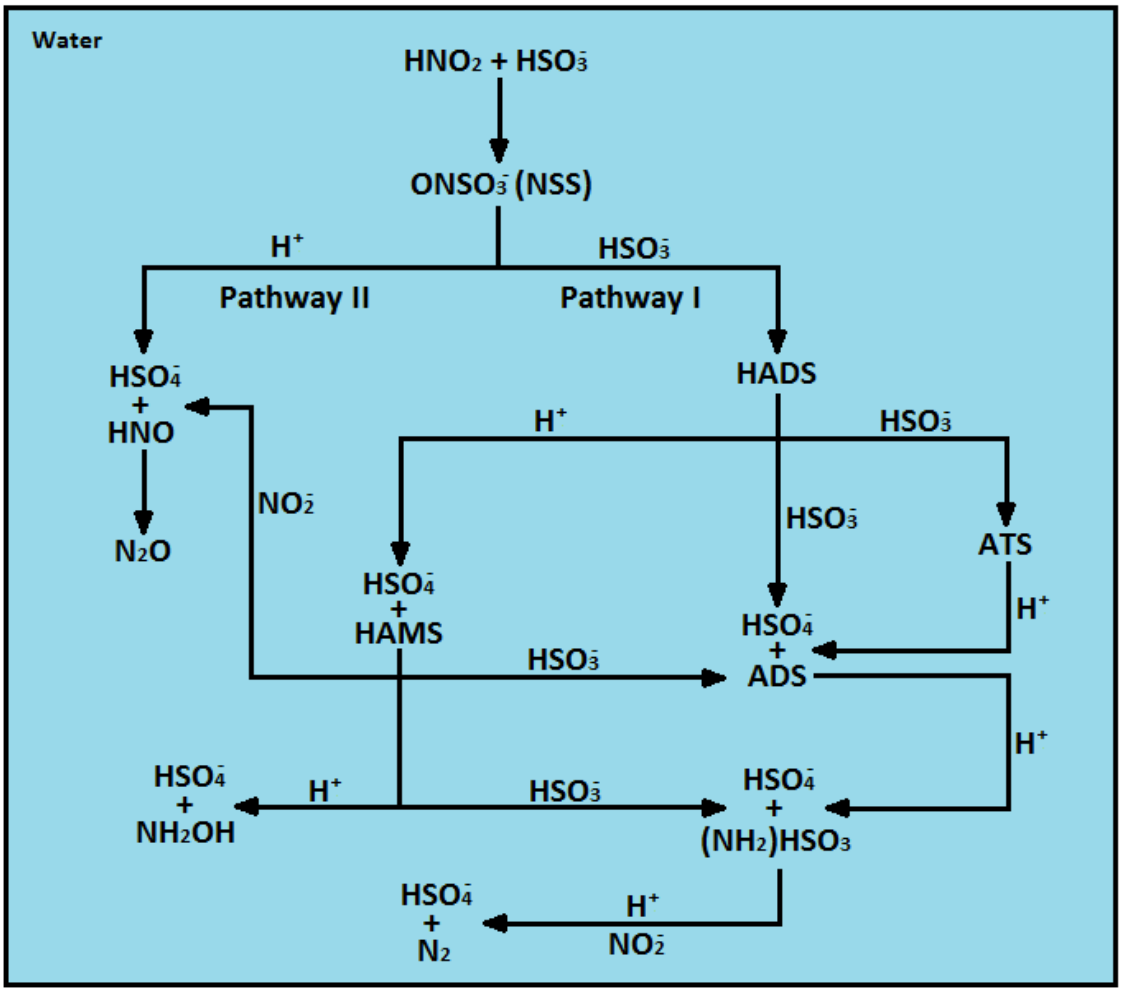

Figure 2.4: A more advanced reaction diagram of pathway I and II compared to Figure 2.3 for the interaction between HNO_2 and HSO_3^- that occurs in the liquid phase of the scrubber. This is an updated version of a reaction diagram done by Ajdari et al. [4].

2.7 Mechanism of absorption

The removal efficiency of NO_x and SO_2 are very dependent on the ability of the gas to be absorbed by the liquid. The rate of the absorption mechanism can be described by the two-film theory. The rate of absorption by diffusion depends on the partial pressure in the gas phase and on the concentration gradient in the liquid phase. It also depends on the interface area where the diffusion is supposed to happen. How the partial pressure/concentration profile for the soluble molecule A looks can be seen in Figure 2.5. Component A will first have to diffuse from the main bulk of the gas through the gas film boundary layer and into the gas film. The concentration in the films on both sides of the interface are in equilibrium and the

resistance to transfer from gas to liquid are mainly centered in that location. From the liquid film component A will enter the main bulk of the liquid through the liquid film boundary layer. The absorption mechanism is reversible and component A will absorb and desorb at the same time.

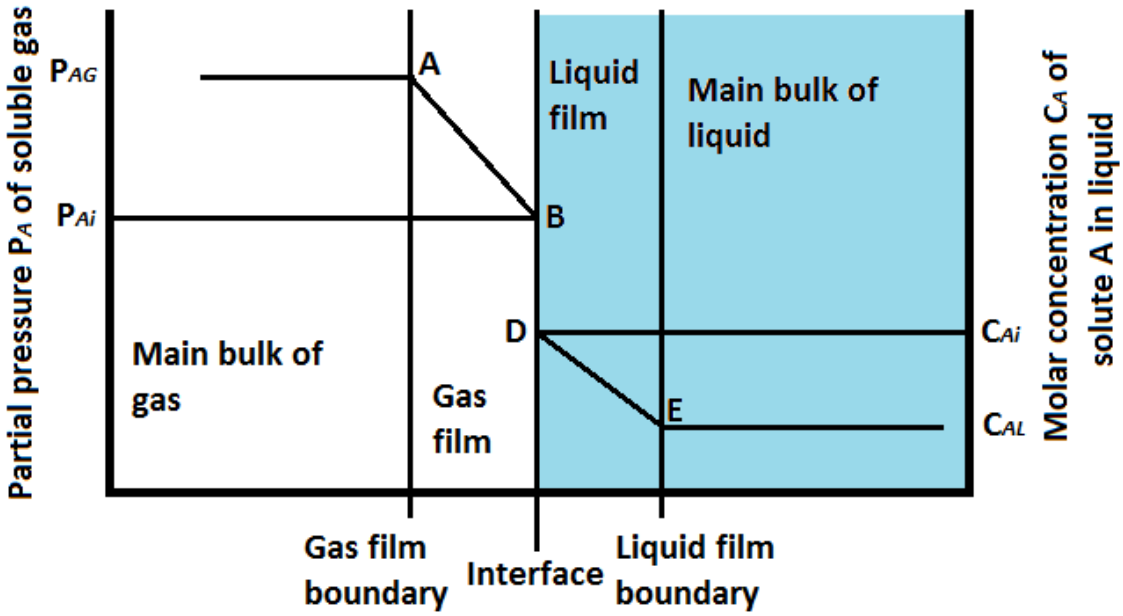

Figure 2.5: Partial pressure/concentration profile for the soluble molecule A.

In Figure 2.5, P_{AG} represents the partial pressure in the bulk of the gas phase, P_{Ai} is the partial pressure at the interface, C_{AL} is the concentration in the bulk of the liquid phase and C_{Ai} is the concentration at the interface.

The rate of mass transfer for gas absorption of a soluble component A in an insoluble component B in the gas phase can be seen in Equation 2.1, according to Stefan's law. N'_A is the overall rate of mass transfer, D_v is the gas-phase diffusivity, z is the distance of mass transfer and C_A, C_B and C_T are the concentration of component A, component B and total bulk of gas.

$$N'_A = -C_T \frac{D_v}{C_B} * \frac{dC_A}{dz} \tag{2.1}$$

The diffusion of the gas in the liquid phase has a lower rate compared to the rate of diffusion in the gas phase. The rate of mass transfer for gas absorption of a soluble component A in the liquid phase can be calculated in a similar way as in the gas phase, according to Equation 2.2.

N'_A is the overall rate of mass transfer, D_L is the diffusivity in the liquid phase, C_A is the concentration of component A and z is the thickness of the liquid phase [11].

$$N'_A = -D_L * \frac{dC_A}{dz} \tag{2.2}$$

Another way of describing the gas absorption from gas to liquid phase is by Henry's law. Henry´s law is the method used in Aspen Plus to describe the solubility of a gas in water. The law describes that the solubility of a gas in a liquid is equal to the partial pressure of the gas above the liquid [12]. Henry´s law is stated in Equation 2.3. C describes the solubility of the gas, k is the Henry´s law constant and P_{gas} is the partial pressure of the gas [12].

$$C = k * P_{gas} \tag{2.3}$$

2.8 Reactions and reaction parameters

There will be different reactions occurring in the ClO_2-reactor compared to the scrubber. The main purpose of the ClO_2-reactor is to oxidize NO to NO_2, because of the higher solubility of NO_2 in water. The liquid from the scrubber will be re-circulated with the purpose of removing more SO_x and NO_x. Equilibrium reactions between the different species and the dissociation of NaOH will occur in the pipes and process equipment spontaneously.

2.8.1 ClO_2-reactor reactions

In the ClO_2-reactor the same reactions will occur through the entire reactor. The reactions are simple compared to the reactions in the scrubber. In the ClO_2-reactor the reactions will only occur in the gas phase. The reactions that occur in the ClO_2-reactor are shown in Table 2.1. The table also shows the kinetics and activation energies.

Table 2.1: Gas-phase reactions in the ClO_2-reactor that will be evaluated in the process in Aspen Plus at a reference temperature of $25°C$.

Reaction	**k** $(m^3 kmole^{-1} s^{-1})$	**n**	**E** $Jmole^{-1}$	**#**	**Reference**
$NO(g) + ClO_2(g) \rightarrow NO_2(g) + ClO(g)$	$6.62 * 10^7$	-	-2910	(2.1.1)	[13]
$NO(g) + ClO(g) \rightarrow NO_2(g) + Cl(g)$	$3.73 * 10^9$	-	-2450	(2.1.2)	[13]
$2ClO(g) \rightarrow ClO_2(g) + Cl(g)$	$2.11 * 10^8$	-	11391	(2.1.3)	[13]
$SO_2(g) + ClO(g) \rightarrow SO_3(g) + Cl(g)$	2409	-	-	(2.1.4)	[14]
$2Cl(g) \rightarrow Cl_2(g)$	$5.8 * 10^8$ $(m^6 kmol^{-2} s^{-1})$	-	0	(2.1.5)	[15]
$2ClO(g) \rightarrow Cl_2(g) + O_2(g)$	$9.21 * 10^8$	-	10293	(2.1.6)	[16]

2.8.2 Scrubber reactions

In the scrubber there are both reactions that are not dependent on the pH and reactions that depend on the different pH, which are stated in Section 2.5. There is both kinetic and equilibrium reactions that occur in the scrubber. For the kinetic reactions that are not dependent on the pH, the kinetics and activation energies are shown in Table 2.2. Table 2.3 shows a list of the equilibrium reactions that are not dependent on pH and their equilibrium constants. The different reactions that occur in the scrubber due to variations in the pH are shown in Table 2.4. The kinetics, activation energies and the specific pH that these reactions occurs at are also shown in Table 2.4.

Table 2.2: Kinetic reactions not depending on pH in the scrubber that will be evaluated in the process in Aspen Plus.

Reaction	k ($m^3 kmole^{-1} s^{-1}$)	n	E ($Jmole^{-1}$)	#	Reference
$2NO_2(aq) + 2H_2O(l) \rightarrow HNO_2 + NO_3^- + H_3O^+$	$1 * 10^8$	-	-	(2.2.1)	[17]
$2HNO_2(aq) \rightarrow NO(aq) + NO_2(aq) + H_2O(l)$	13.4	-	-	(2.2.2)	[18]
$NO(aq) + NO_2(aq) + H_2O(l) \rightarrow 2HNO_2(aq)$	$1.6 * 10^8$	-	-	(2.2.3)	[18]
$2NO(g) + O_2(g) \rightarrow 2NO_2(g)$	1197 ($m^6 kmol^{-2} s^{-1}$)	-	-4409.7	(2.2.4)	[19]

Table 2.3: Equilibrium reactions not depending on pH in the scrubber that will be evaluated in the process in Aspen Plus.

Reaction	A	B	C	D	#	Reference
$2H_2O(l) \leftrightarrow H_3O^+(aq) + OH^-(aq)$	132.899	-13445.9	-22.4773	0	(2.3.1)	[20]
$SO_2(aq) + 2H_2O(l) \leftrightarrow H_3O^+(aq) + HSO_3^-(aq)$	-5.97867	637.396	0	-0.0151337	(2.3.2)	[21]
$HNO_2(aq) + H_2O(l) \leftrightarrow H_3O^+(aq) + NO_2^-(aq)$	-11.5926	0	0	0	(2.3.3)	[18]
$HSO_3^-(aq) + H_2O(l) \leftrightarrow H_3O^+(aq) + SO_3^{2-}(aq)$	-25.2906	1333.4	0	0	(2.3.4)	[22]

Table 2.4: pH depending reactions in the scrubber and at what pH they occur at.

pH	Reaction	k ($m^3 kmole^{-1} s^{-1}$)	n	E ($Jkmole^{-1}$)	#	Reference
1	$HNO_2(aq) + HSO_3^-(aq) \rightarrow 0.5N_2O(aq) + HSO_4^-(aq) + 0.5H_2O(l)$	$1.11 * 10^9$	0	$5.07521 * 10^7$	(2.4.1)	[23]
2	$HNO_2(aq) + 2HSO_3^-(aq) \rightarrow HADS(aq) + H_2O(l)$	$1.887 * 10^9$	0	$5.07521 * 10^7$	(2.4.2)	[23]
	$HNO_2(aq) + HSO_3^-(aq) \rightarrow 0.5N_2O(aq) + HSO_4^-(aq) + 0.5H_2O(l)$	$1.11 * 10^9$	0	$5.07521 * 10^7$	(2.4.1)	[23]
4	$HNO_2(aq) + 2HSO_3^-(aq) \rightarrow HADS(aq) + H_2O(l)$	$1.887 * 10^9$	0	$5.07521 * 10^7$	(2.4.2)	[23]
5-7	$HNO_2(aq) + 2HSO_3^-(aq) \rightarrow HADS(aq) + H_2O(l)$	$1.887 * 10^9$	0	$5.07521 * 10^7$	(2.4.2)	[23]
	$2NO_2(aq) + HSO_3^-(aq) + H_2O(l) \rightarrow 2HNO_2(aq) + HSO_4^-(aq)$	$1.24 * 10^7$	0	0	(2.4.3)	[24]
8-13	$2NO_2(aq) + HSO_3^-(aq) + H_2O(l) \rightarrow 2HNO_2(aq) + HSO_4^-(aq)$	$1.24 * 10^7$	0	0	(2.4.3)	[24]

2.8.3 Overall equilibrium and dissociation reactions

Equilibrium reactions between some species will occur in the pipes and process equipment over the whole process. The equilibrium reactions and the constants are showed in Table 2.5. The dissociation of NaOH will occur spontaneously when it meets the water after the injection.

Table 2.5: Equilibrium reactions that will occur in the pipes and process equipment and the dissociation of NaOH. For the reactions that has no values in the table, Aspen Plus will compute the equilibrium constants from Gibbs energies and use during the simulation.

Reaction	**A**	**B**	**C**	**D**	**#**	**Reference**
$2H_2O(l) \leftrightarrow H_3O^+(aq) + OH^-(aq)$	132.899	-13445.9	-22.4773	0	(2.5.1)	[20]
$SO_2(aq) + 2H_2O(l) \leftrightarrow H_3O^+(aq) + HSO_3^-(aq)$	-5.97867	637.396	0	-0.0151337	(2.5.2)	[21]
$HNO_2(aq) + H_2O(l) \leftrightarrow H_3O^+(aq) + NO_2^-(aq)$	-11.5926	0	0	0	(2.5.3)	[18]
$CO_2(aq) + 2H_2O(l) \leftrightarrow H_3O^+(aq) + HCO_3^-(aq)$	231.465	-12092.1	-36.7816	0	(2.5.4)	[20]
$HCO_3^-(aq) + H_2O(l) \leftrightarrow H_3O^+(aq) + CO_3^{2-}(aq)$	216.05	-12431.7	-35.4819	0	(2.5.5)	[20]
$H_2SO_4(aq) + H_2O(l) \leftrightarrow H_3O^+(aq) + HSO_4^-(aq)$	-	-	-	-	(2.5.6)	-
$HSO_4^-(aq) + H_2O(l) \leftrightarrow H_3O^+(aq) + SO_4^{2-}(aq)$	-	-	-	-	(2.5.7)	-
$HNO_3(aq) + H_2O(l) \leftrightarrow H_3O^+(aq) + NO_2^-(aq)$	-	-	-	-	(2.5.8)	-
$NaOH \rightarrow Na^+(aq) + OH^-(aq)$	-	-	-	-	(2.5.9)	-

3

Method

The methodology of this master thesis was to first create a simulation model in Aspen Plus. The model will be evaluated by simulating certain cases, to see if the behaviour of the model is reasonable compared to the expectations and previous models. Different cases are then simulated to see how the simultaneous removal efficiency of S/NOx are affected. From those simulations the results will be used to recommend an experimental plan for the technical scale experiments.

3.1 Model in Aspen Plus

The process simulation model in Aspen Plus is developed to simulate the technical scale experiments setup in the Chalmers 100 kW oxy-fuel unit, showed in Figure 2.1. Due to restrictions in Aspen Plus that will be described in this chapter, where the model created as in Figure 3.1. The differences between the model created in Aspen Plus compared to the technical scale experiment setup, was the addition of another cooler to simulate the decrease in temperature in the scrubber due to the lack of isolation and the addition of purge and makeup streams in the recycle loop, to simulate the process tank due to convergence errors in Aspen Plus. The main part of the project is directed to the scrubber and most of the work has been focused on that particular process block because of the complex chemistry in it.

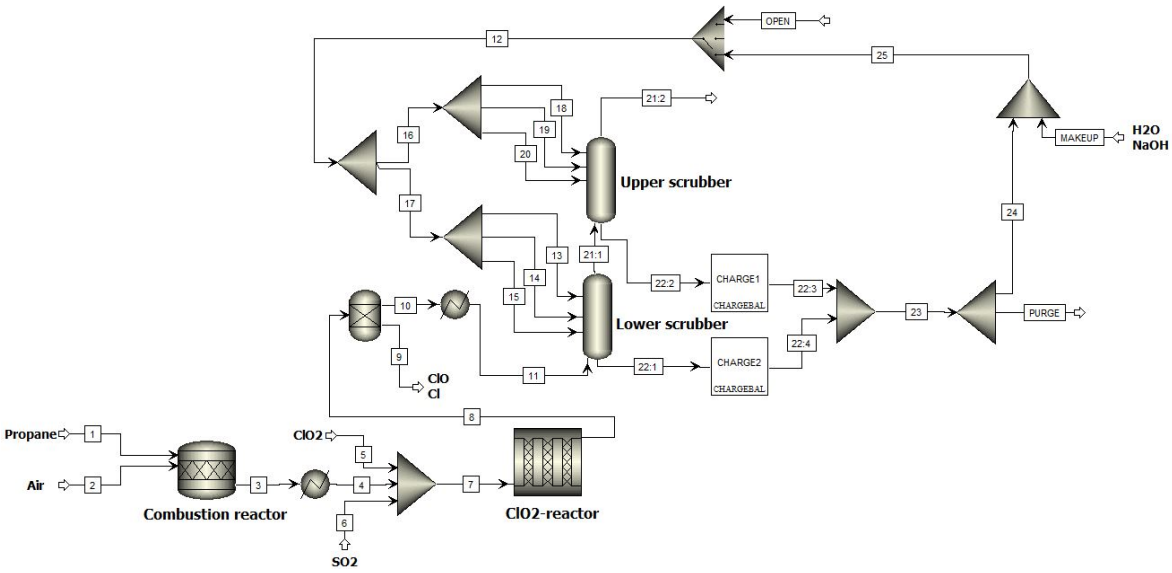

Figure 3.1: Overview of the model in Aspen Plus.

3.1.1 Property setup in Aspen Plus

The chemistry in the model is defined as an electrolyte system. Aspen Plus solves these systems by partially or completely dissociate certain molecular species into ions in the solvent. The dissociation is described by liquid phase equilibrium reactions and is referred in Aspen Plus as the solution chemistry or just as Chemistry. In a nonelectrolyte system, the chemical reactions only occur in reactors, but in an electrolyte system, the dissociation occurs as fast as the electrolytes get in contact with the liquid solvent. By using the Chemistry input in Aspen Plus all pipes and unit operation blocks will be able to handle the electrolyte reactions. The equilibrium reactions and the dissociation that is inserted in the Chemistry are shown in Table 2.5. The model used in Aspen Plus for solving these electrolyte calculations is the Electrolyte-NRTL activity model (ELECNRTL). ELECNRTL calculates the liquid phase properties by using an activity coefficient model and the vapor phase properties comes from the Redlich-Kwong equation of state.

Due to the high interactions between gas and liquid in this model (especially in the scrubber) it is necessary to include the Henry Comps Global input into the simulation. This model uses Henry's law to decide the equilibrium components between the gas and liquid phase.

The property database in Aspen Plus is used for all molecules except hydroxylamine disulfonic acid (HADS) which is missing, the molecular formula can instead be drawn which Aspen Plus will calculate parameters based on.

The solvent pH is important to the chemistry and calculated to be able to run the scrubber in a correct way, it is important to be able to calculate the pH profile inside

it. This can be done by inserting pH as a physical property under Property Sets and then choosing it under Analysis when running the scrubber.

3.1.2 Simulation setup in Aspen Plus

Figure 3.1 shows the flowsheet that was created in Aspen Plus. The flowsheet contains the streams and model blocks connected to each other. All inlet streams require two thermodynamic specifications such as temperature and pressure. The pressure will be atmospheric for the whole model. The inlet streams also require the flow rate to be specified and what molecules certain streams contain. How and in what order the model blocks are connected can be seen in Figure 3.1, a detailed description on how these blocks were setup are described in the following subsections.

3.1.2.1 Combustion reactor

The combustion of propane is modeled in Aspen Plus as a stoichiometric reactor based on known conversion (RStoic). Propane is used as fuel in the combustion reactor. The fuel flow is calculated from the lower heating value (LHV) for propane which is 46.3 MJ/kg [25] and the capacity of 80 kW is used in the model. The oxy-fuel unit at Chalmers is built for a maximum capacity of 100 kW, but during the technical scale experiments will it be run at about 80 kW. Due to that specification in the technical scale experiments the model is simulated at 80 kW. Oxygen excess is used in the combustion reactor, with a lambda value of 1.15. Propane is simulated with a conversion degree of 100 %. The two reactions that takes place in the reactor are shown in Table 3.1. 300 ppm of NO_x is wanted into the scrubber and the temperature that is used in the reactor is 800 °C.

Table 3.1: Reactions that occurs in the combustion reactor.

Reaction
$C_3H_8 + 5O_2 \rightarrow 3CO_2 + 4H_2O$
$5,5N_2 + 6O_2 \rightarrow 10NO + NO_2$

3.1.2.2 ClO_2-reactor

A heat exchanger is used after the combustion reactor to decrease the temperature of the exhaust gas from 800 °C to 200 °C. Before the ClO_2-reactor SO_2 will be added to be able to simulate the model with SO_2 in it, since SO_2 is not produced during the combustion of propane. This will also be done in a similar way during the technical scale experiments. Different amount of SO_2 into the scrubber are tested. ClO_2 will be added into the ClO_2-reactor. The reactor will be modeled in Aspen Plus as a plug flow reactor (RPlug). The purpose of the ClO_2-reactor is to oxidize NO to NO_2, since NO_2 is more soluble in water. In the real case (technical scale experiments) the oxidation of NO will take place in the pipe into the scrubber, how this looks

like can be seen in A.3. The length of the ClO_2-reactor is 0.9 m, the diameter is 0.1 m in the start and end point and 0.2 m in the middle. In Table 2.1 the reactions that occur in the ClO_2-reactor, the kinetics and activation energies can be seen.

Both ClO and Cl are produced in the ClO_2-reactor from the reactions, see Table 2.1. To be able to run the model after the ClO_2-reactor, both those species had to be removed. This will not affect the results because of the small amount of the two species. The reason for this is that Aspen Plus has missing parameters for those species and is not able to solve the heat balances. Heat balances are necessary for further simulations.

3.1.2.3 Scrubber

The scrubber is simulated as two RadFrac towers in Aspen Plus since the scrubber in the experiments is divided into two sections, as desbrided in Chapter 2.4 and Figure 2.2. Both of the scrubber sections have three inlets with water, see Figure 3.2. The scrubber sections are simulated with 15 theoretical stages each, 30 in total. 15 stages was used because more are not necessary and give approximately the same results. The benefits with more stages are that it is easier to place the water inlet streams at the right position and that the shapes of the composition graphs will be better due to smaller intervals. The water inflows are connected in the same way for both scrubber sections, at stage 1, 4 and 6. The exhaust gas enters the bottom part of the lower scrubber section and flows in a counter current direction to the liquid water. From the top of the lower scrubber section the exhaust gas will exit and enter the second scrubber. The exhaust gas flows from the bottom to the top in the upper scrubber section. The temperature of the flue gas is decreased to 25 °C before it enters the scrubber. The reason for this is that the temperature in the scrubber will be in equilibrium with the surrounding temperature in the real case, because of the lack of isolation in the scrubber. The cooling of the exhaust gas flow will correspond to approximately an effect of 12 kW. Figure 3.2 can be compared with Figure A.3, to see how the scrubber looks like in reality.

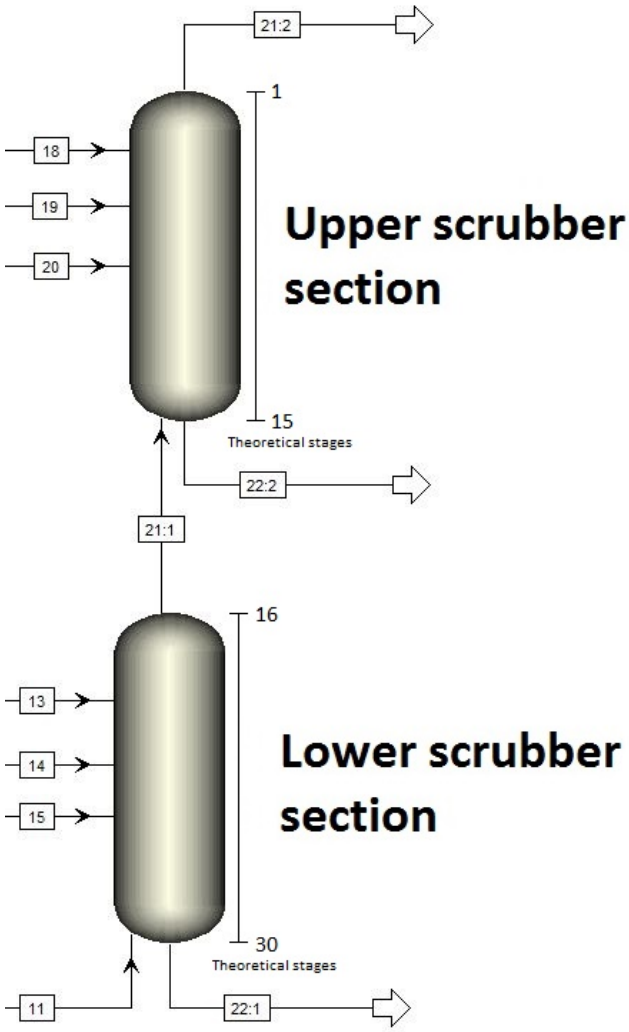

Figure 3.2: From Figure 3.1 in Chapter 3.1, scrubber model in Aspen Plus.

A spray column unit is not possible to choose in Aspen Plus, therefore a packed column is selected with low packing factor and high void fraction. A packed column with low packing factor and high void fraction are similar to a spray column. The specifications for the scrubber is shown in Table 3.2. Different void fractions are investigated and tested in Aspen Plus. The void fraction has not that big impact on the result. For a void fraction between 0.85-1 was the result similar, that is the reason why 0.88 was used.

Table 3.2: Specifications in the scrubber used in Aspen Plus.

Parameter	**Lower Scrubber**	**Upper Scrubber**
Calculation type	Rate-Based	Rate-Based
Number of theoretical stages	15	15
Valid phases	Vapor-Liquid	Vapor-Liquid
Pressure [atm]	1	1
Specification type	Packing Rating	Packing Rating
Section diameter [m]	0.26	0.26
Height [m]	2.62	2.12
Packing factor [1/m]	72.2	72.2
Void fraction $[m^2/m^3]$	0.88	0.88

In Aspen Plus it is possible to specify what reaction that will happen in the scrubber and at which stages they will be active. The latter is an important aspect to consider, because different reactions will occur at different pH and the pH will vary along the scrubber, Chapter 2.4. Table 2.2 and 2.3 shows reactions that occurs all across the scrubber and not at a certain pH. Only the important reactions have been added to the scrubber, other reactions have been tested and seen as negligible. Would only give more convergence problems for little results.

In Table 2.4 the reactions that occur at certain pH can be seen. The pH and the corresponding reactions are divided into a few intervals that covers the entire pH profile of the scrubber.

3.1.2.4 Recycle loop

The recycle loop and process tank in the Chalmers 100kW oxy-fuel unit is simulated in Aspen Plus according to Figure 3.3. The recycle loop contains; mixers, splitters and charge balance blocks. A completely closed liquid loop can not be simulated in Aspen Plus, due to problems with accumulation of the liquid. To solve this problem a purge and makeup stream has been introduced according to Figure 3.3. The liquid stream out of the scrubber will be splitted and a part of the flow will leave the model as the purge stream. The makeup stream will then be added, the molar flow of that will be iterated by hand to match the purge stream. If the purge and makeup stream not are matched, the model will run dry or give incorrect liquid to gas ratio. In the makeup stream NaOH solved in water will be introduced to the model. NaOH is introduced to reach the desired pH of the liquid going into the scrubber.

To know how much of the flow that should leave the model in the purge stream, different cases were tested. The different cases that were tested was to remove 0-100 % of the flow. When 0 % was removed Aspen Plus cannot handle the simulation. The lowest case that Aspen Plus could simulate was when removing 10 %. The

removal efficiency increased with a negligible level when gradually increasing the purge to 100 % compared to 10 %. 10 % gave a good removal efficiency of both NO_x and SO_2 and because of that 10 % was used.

In the real process during the technical scale experiments, it can take one hour for the liquid to recirculate back into the scrubber. To simulate this recirculating time in Aspen Plus a batch reactor was used in the recycle loop with the residence time of one hour. No chemical was added in the batch reactor and the temperature was constant at 25 °C. The reason to use the batch reactor was to investigate if the residence time would affect the liquid equilibrium reactions. With the added batch reactor, the species in the liquid have longer time to react according to the equilibrium reactions in Table 2.5. The results given from that simulation was similar to a case without the batch reactor. This means that the longer recirculating time did not affect the efficiency of the liquid equilibrium reactions and it can be neglected.

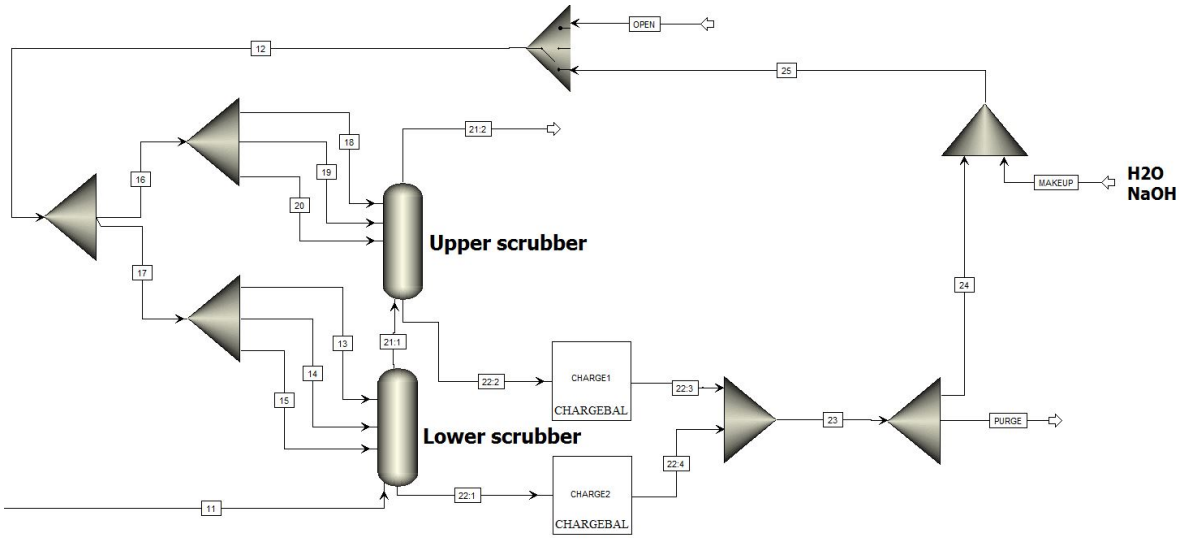

Figure 3.3: Overview of the recycle loop in Aspen Plus, from Figure 3.1 in Chapter 3.1.

The Wegstein solver that is used in this project to solve the recycle loop, might vary the flow of different ionic species in the tear stream in different ways. That can then cause charge balance problems in the simulation. To solve this problem two charge balance blocks are used to enforce electroneutrality after the scrubbers. The tear stream contains start guesses of the specifications required for a stream and is used to help converging the recycle loop. Stream 12 in Figure 3.3 is the tear stream in this model.

Aspen Plus is more sensitive when the model is simulated as closed compared to open. The program might have problems with convergence errors. To solve this problem the model is first simulated as open to give Aspen Plus good initial guesses. Then the model can be simulated as closed with the good initial guesses and is not

that sensitive. This can be done by inserting a Selector block. The Selector can choose what inlet stream that should be used in the model. How the Selector is connected can be seen in Figure 3.3.

3.2 Evaluation of the model

The evaluation of the model is done to see if the behaviour of the model is reasonable compared to the expectations and previous models. The cases simulated are; pure SO_2, NO_2, NO and the mixture S/NO_x into the scrubber, see Table 3.3.

Table 3.3: The cases simulated to evaluate the model.

Species present in gas inlet	**pH**	**l/g**
Pure SO_2	10	8 and 5
Pure NO_2	10	8
Pure NO	10	8
SO_2, NO_2 and NO	10	8

The first evaluation made was to see the behaviour of the scrubber when there was only SO_2 and no NO_2 or NO in the inlet to the scrubber. To be able to simulate this case, the reaction which produces NO and NO_2 from N_2 in the combustion reactor and the ClO_2-reactor was removed from the model. To be able to run this case, different parameters like the NaOH concentration and specific reactions were adjusted in the model. For pure SO_2 two different cases were tested. For both cases, the same pH value into the scrubber was used but different liquid to gas ratio (l/g). l/g is defined as the ratio between the liquid flow into the scrubber in l/s and the gas flow into the scrubber in m^3/s. The reason that two different l/g were tested was because it will then be easier to compare it with other models in Table A.2, when both SO_2 and NO_x are present.

The second evaluation that was done of the model was to see the behaviour of NO_2 in the scrubber when there was no NO or SO_2 present. To be able to simulate this case, the injection stream of SO_2 was removed. All the NO was oxidized to NO_2 in the ClO_2-reactor.

The third evaluation of the model that was done, was to see the behaviour of NO in the scrubber when no SO_2 or NO_2 was present. This case was simulated by changing the reaction in the combustion reactor to only produce NO.

The final evaluation of the model was done on a S/NO_x case. The exhaust gas contained; SO_2, NO_2 and NO according to the specifications. There is a lack of knowledge about the chemistry that will occur in the scrubber, because it is a new field of research. That makes it hard to evaluate the whole model, instead things

like, convergence stability and reaction rates was investigated and compared to available literature. This case was simulated according to Figure 3.1.

The outlet parameters that was analyzed was the amount of removed SO_2 and NO_x, pH in the outlet, ratio nitrite/nitrate and sulfite/sulfate. The standard amount of SO_2 and NO_x was used in the inlet to the scrubber which are 500 ppm and 300 ppm respectively.

3.3 Cases

The aim with this master thesis is to simulate different cases with the model to see how the simultaneous removal efficiency of S/NO_x are affected. From those simulations the results will be used to recommend an experimental plan for the technical scale experiments. The main parameters that was varied were the l/g and the pH into the scrubber.

The different l/g that were simulated in the model were 8 and then decreased in intervals to the lowest ratio that the model could handle which is 2.5. Those different cases are simulated by adjusting the start guess in the makeup and the tear stream. For each case the reactions in the scrubber and the concentration of NaOH were adjusted. The specific pH into the scrubber varied for the different l/g. Different pH values were tested, 10 as highest and then down to self buffering. To simulate the lowest pH all the NaOH in the makeup stream was removed. Different amounts of ppm values of SO_2 and NO_x was used in the gas inlet. To see the effect of the sulfite concentration in the liquid inlet to the scrubber and how it affects the reactions in Table 2.4 was also simulated. It was simulated by addition of sulfite in the makeup stream until the desired concentration into the scrubber were reached. Three different l/g were simulated, but all with the same pH into the scrubber. Those cases were then compared to cases with the same l/g and pH but with no sulfite in the liquid inlet. That was achieved by running the simulation as an open liquid loop and without addition of sulfite in the makeup. The different cases that was simulated are shown in Table 3.4.

Table 3.4: The different cases that was simulated.

SO_2/NO_x in gas inlet	**Sulfite in to scrubber**	**pH**	**l/g**
[ppm]	**[mg/l]**	-	**-**
500/300	Not fixed	10 - self buff.	8 - 2.5
750/300	Not fixed	10 and 4	5
500/300	0 and 3150	10	8 - 2.5

The same outlet parameters as in the evaluation were analyzed. Since SO_2 and NO_x was present in the same model sulfate, N_2O and HADS will also be produced

according to Reaction (2.4.1)-(2.4.3). The standard amount of SO_2 and NO_x was used in the inlet to the scrubber which are 500 ppm and 300 ppm respectively.

For a standard case with pH 10 and 5 l/g were the mole- and mass flows calculated for N, S and H_2O. The balances were represented over the scrubber from Aspen Plus, to validate that the balances were correct.

3.4 Recommendations for experimental validation

From the results in Chapter 4.2 were four cases proposed with different; ratio between SO_2 and NO_x in the gas inlet to the scrubber, pH in the liquid into the scrubber and l/g. These cases were selected specifically to give a high variation in ways to operate the scrubber and the results received. It was also selected to validate the chemistry and see the behaviour of the process in different the cases. The cases will then be used as recommendations for experimental validation during the technical scale experiments in the Chalmers 100 kW oxy-fuel unit.

4

Results

4.1 Evaluation of the model

The evaluation of the model was done through simulations with pure SO_2, NO_2, NO and a mixed S/NO_x case, as described in Chapter 3.2 and Table 3.3. Figure 4.1 shows the removal of SO_2 from the gas phase in the case with pure SO_2, pH 10 and 8-5 l/g.

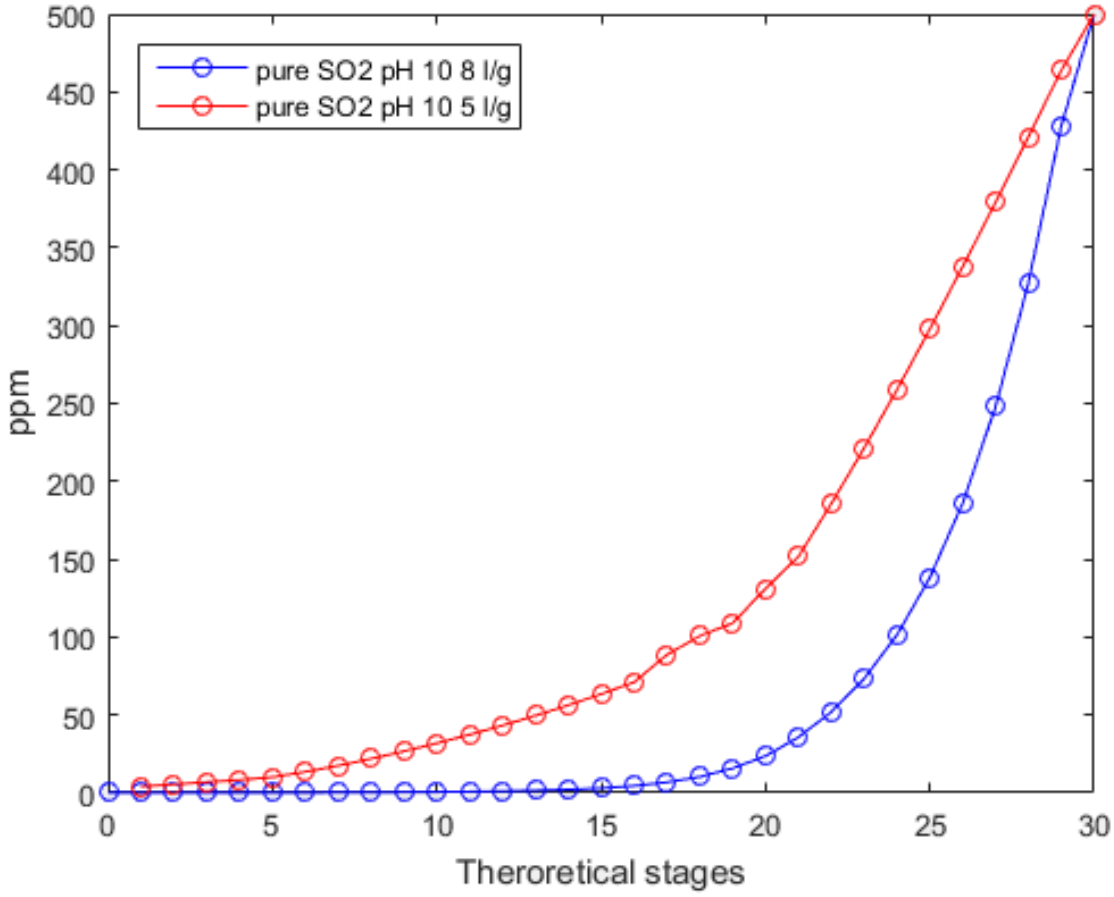

Figure 4.1: Graph on the pure SO_2 case with 8 and 5 l/g, how the vapor mole fraction of SO_2 varies through the scrubber. The flue gas will enter in the bottom of the scrubber at stage 30.

Figure 4.2 shows the simulated case with pure NO_2 into the scrubber, with pH 10 and 8 l/g.

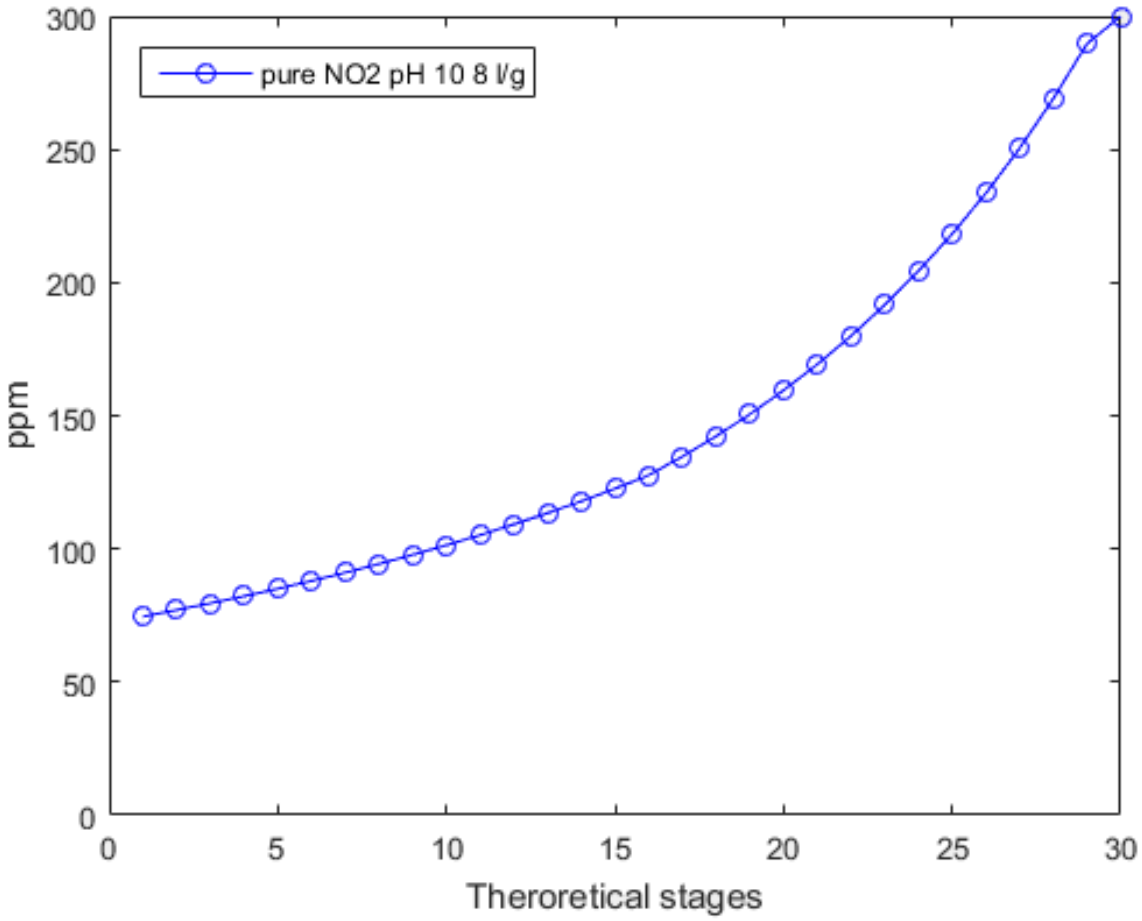

Figure 4.2: Graph on the pure NO_2 case, how the vapor mole fraction of NO_2 varies through the scrubber. The flue gas will enter in the bottom of the scrubber at stage 30.

In Table A.1 in Appendix A.2 can more results from the evaluation be seen.

4.2 Cases

In the figures below, can the results from the simulations to retrieve process parameters for the experimental plan to the technical scale experiments be seen. An overview of the cases that was simulated can be viewed in Table 3.4.

Figure 4.3 shows the removal of SO_2 for the simultaneous S/NO_x case with 8-2.5 l/g and pH 10-self buffering in the inlet to the scrubber.

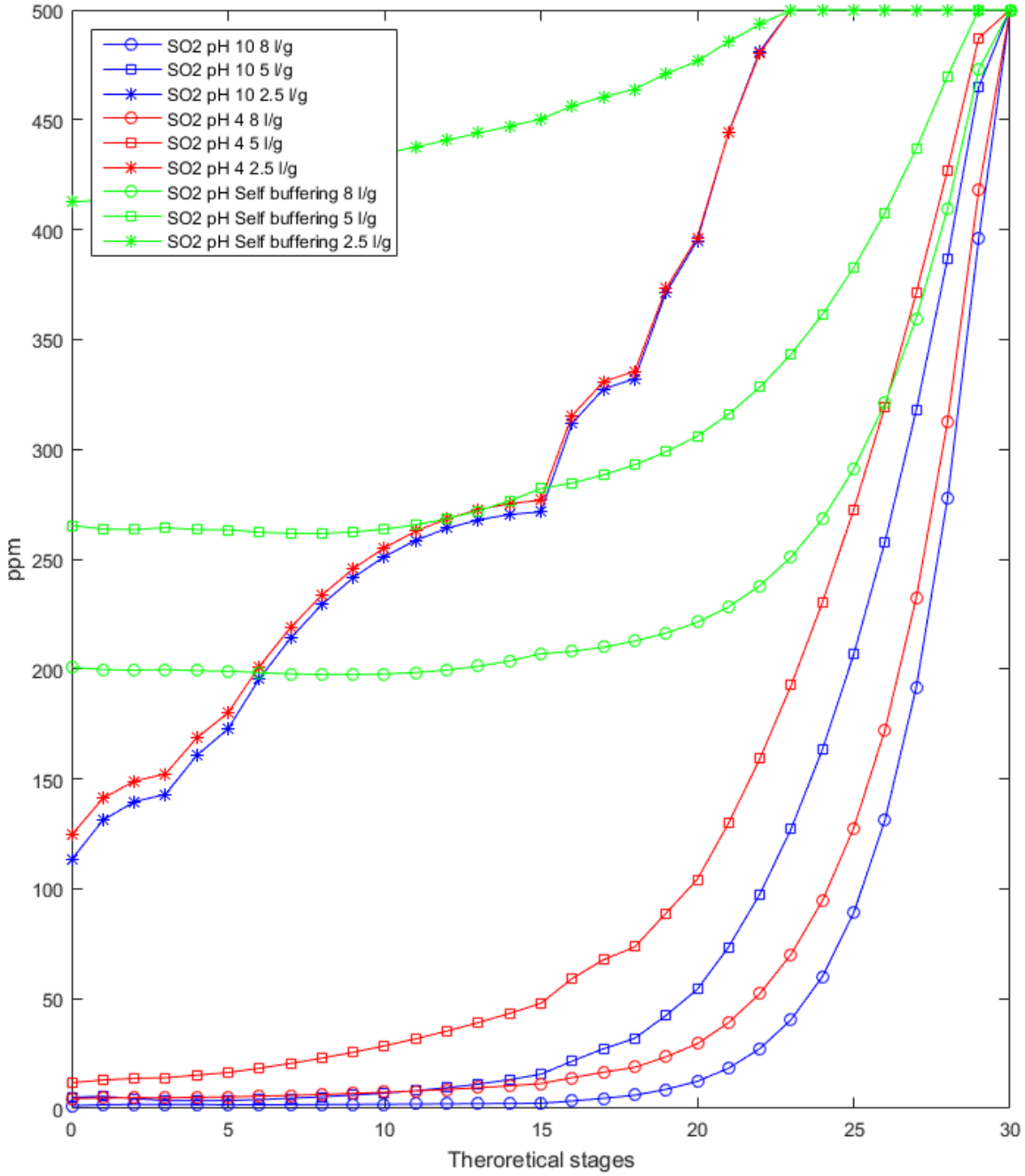

Figure 4.3: Graph on the 8-2.5 l/g S/NO_x case with pH 10-self buffering into the scrubber and how the amount of SO_2 in the vapor phase varies through the scrubber. The flue gas will enter in the bottom of the scrubber at stage 30.

Figure 4.4 shows the removal of NO_x for the simultaneous S/NO_x case with 8-2.5 l/g and pH 10-self buffering in the inlet to the scrubber.

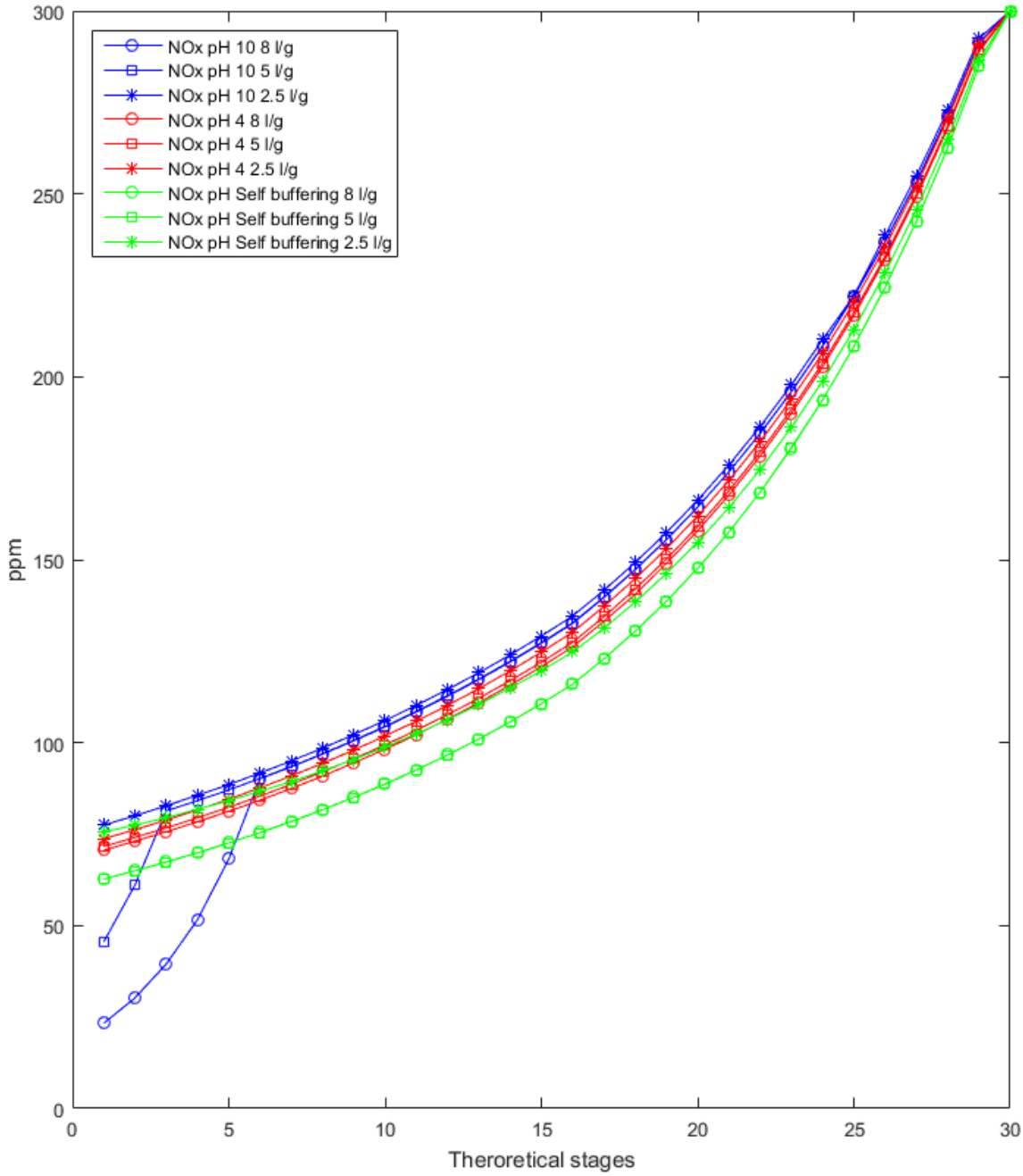

Figure 4.4: Graph on the 8-2.5 l/g S/NO_x case with pH 10-self buffering into the scrubber and how the amount of NO_x in the vapor phase varies through the scrubber. The flue gas will enter in the bottom of the scrubber at stage 30.

In Figures 4.5 and 4.6 the removal efficiency of SO_2 and NO_x from Figure 4.3-4.4 is compiled for the span of pH and l/g.

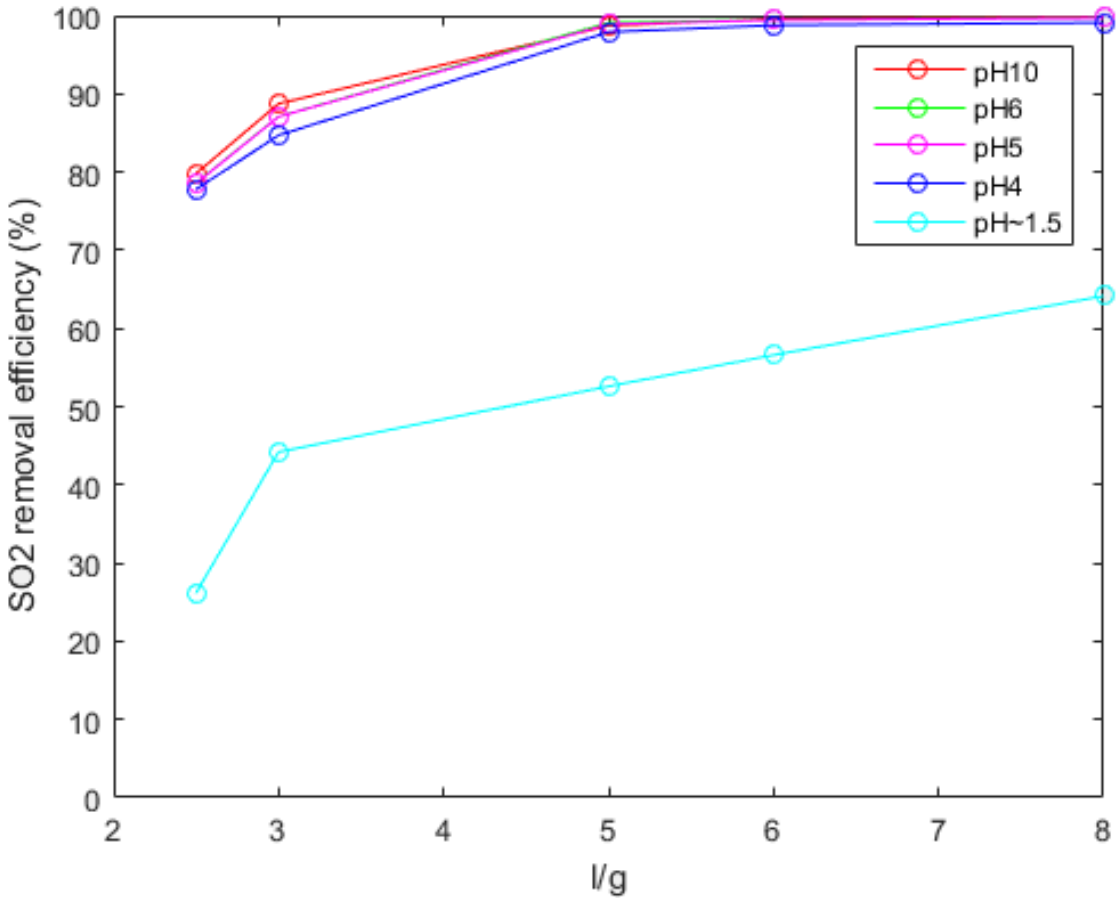

Figure 4.5: Compiled graph containing all S/NO_x cases. It describes how the removal efficiency of SO_2 varies when l/g and pH into the scrubber are varied.

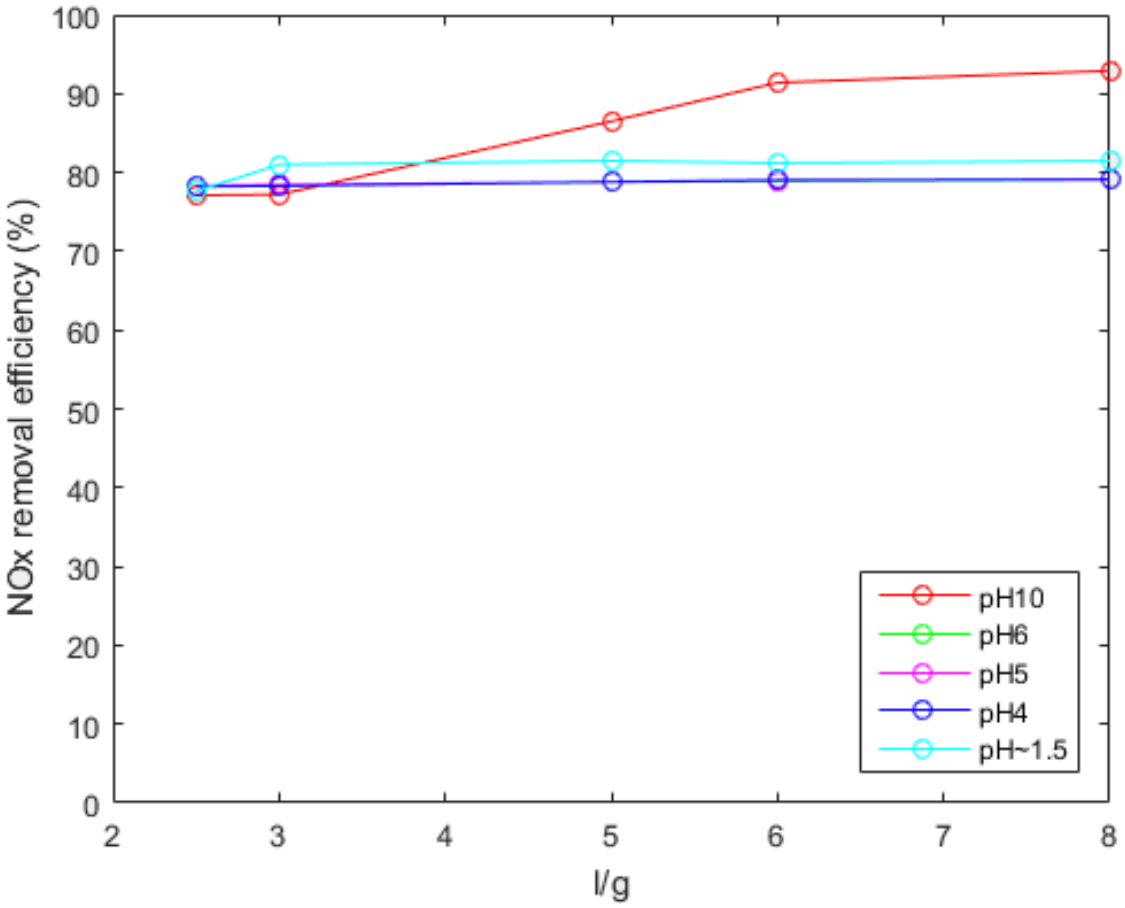

Figure 4.6: Compiled graph containing all S/NO_x cases. It describes how the removal efficiency of NO_x varies when l/g and pH into the scrubber are varied.

Figure 4.7 shows the removal behaviour of SO_2 and NO_x for two simultaneous non-standard S/NO_x cases with 5 l/g and pH 10 and 4 in the inlet to the scrubber.

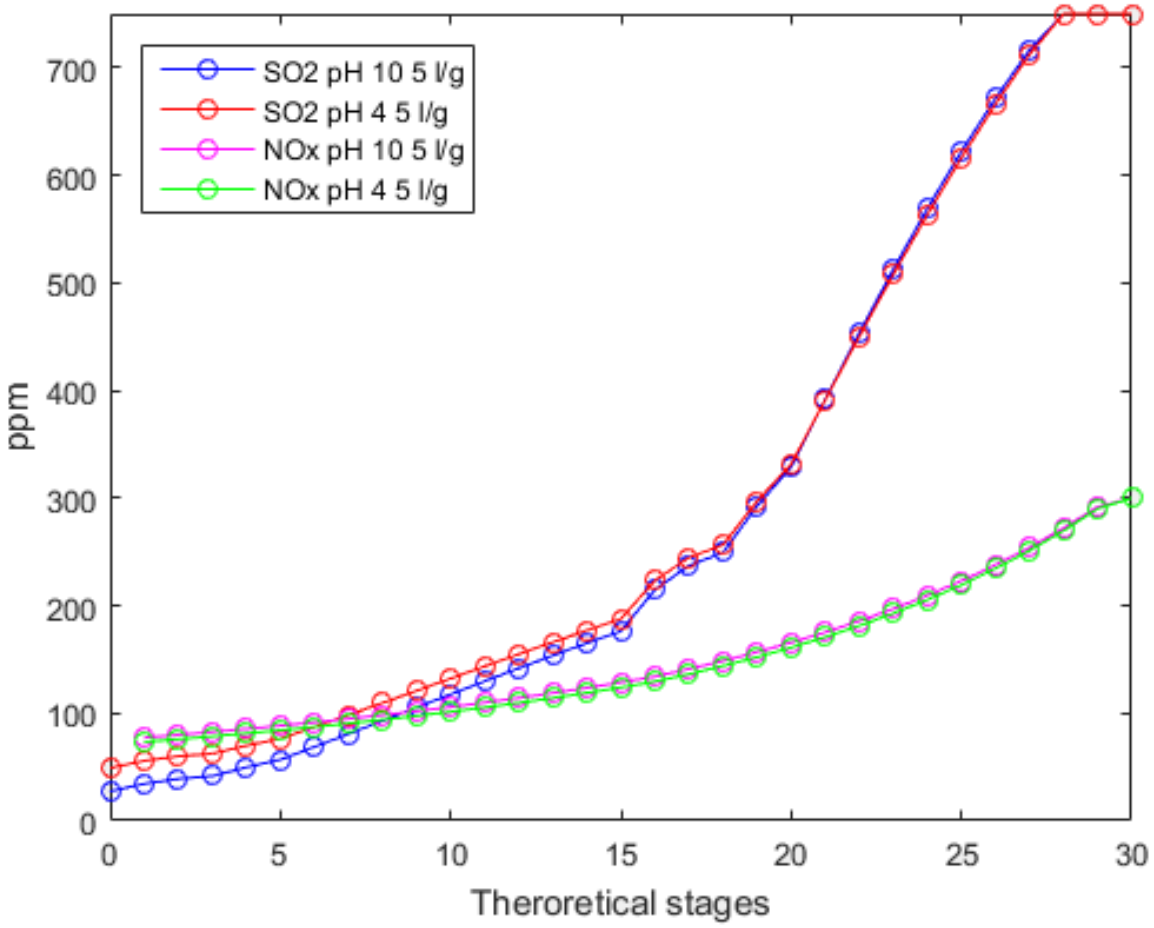

Figure 4.7: Graph on a non-standard S/NO_x case with 750 ppm SO_2 and 300 ppm NO_2 in the inlet to the scrubber. The figure shows two cases for the removal of SO_2 and NO_x, both with 5 l/g and pH 10 and 4. The flue gas will enter in the bottom of the scrubber at stage 30.

Figure 4.8 and 4.9 shows graphs on standard S/NO_x cases with different sulfite concentration into the scrubber and how it affects the removal efficiency of SO_2 and NO_x.

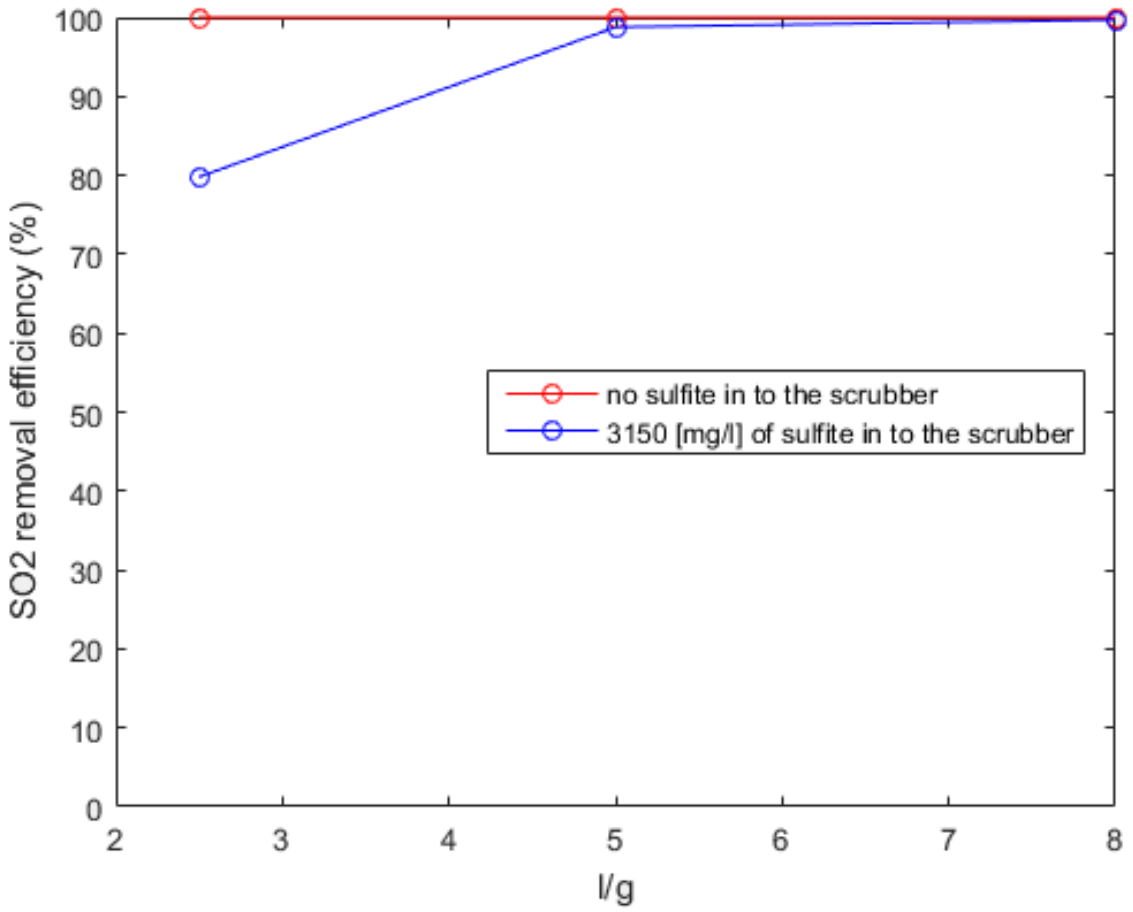

Figure 4.8: Graph on a standard S/NO_x case with different sulfite concentration into the scrubber and how it affects the removal efficiency of SO_2. The pH is 10 into the scrubber and l/g is varied.

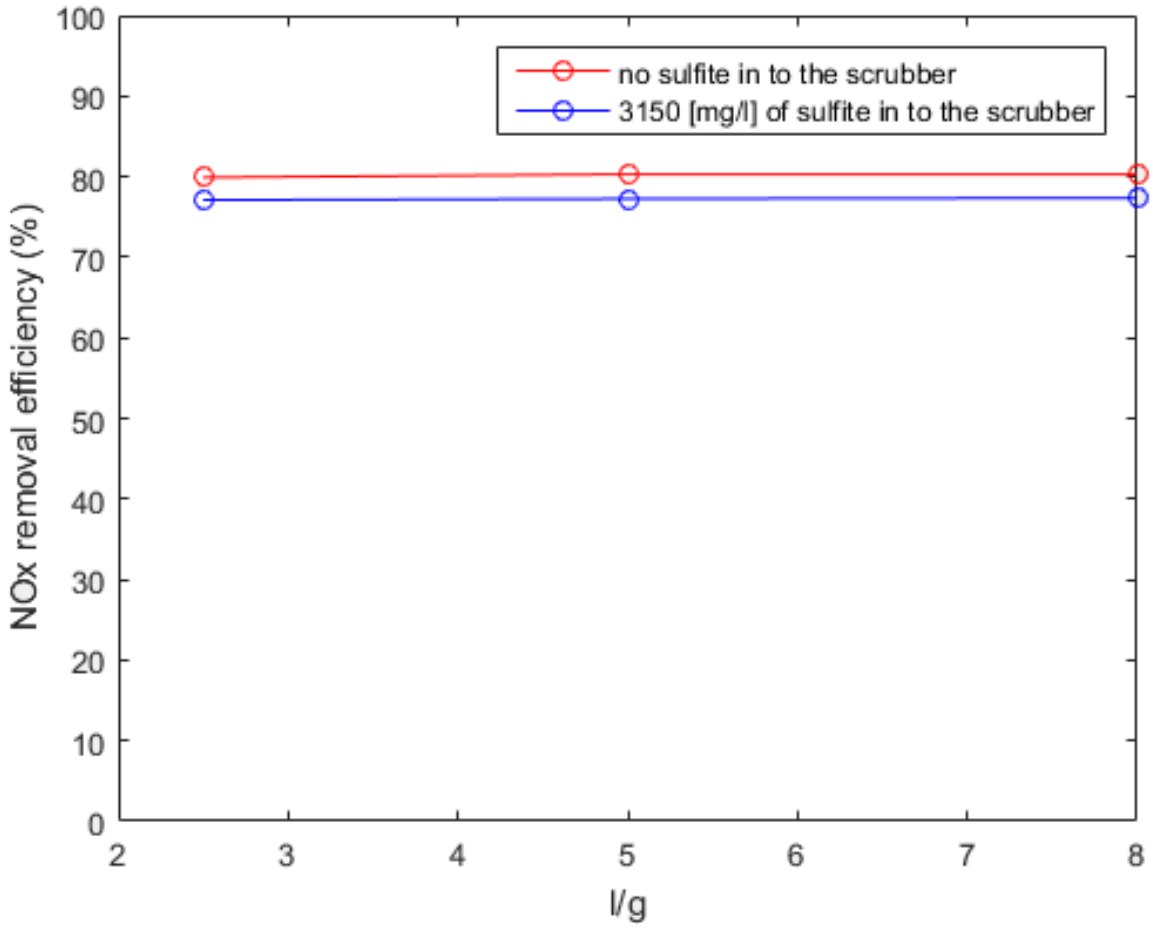

Figure 4.9: Graph on a standard S/NO_x case with different sulfite concentrations into the scrubber and how it affects the removal efficiency of NO_x. The pH is 10 into the scrubber and the l/g is varied.

In Table A.2-A.5 in Appendix A.2 can more results from the cases be seen.

Figure 4.10 shows a simplified overview of the scrubber with a recirculation system. The values of the mole- and mass flows are averaged, this gives that the mole- and mass balances will not be totally correct.

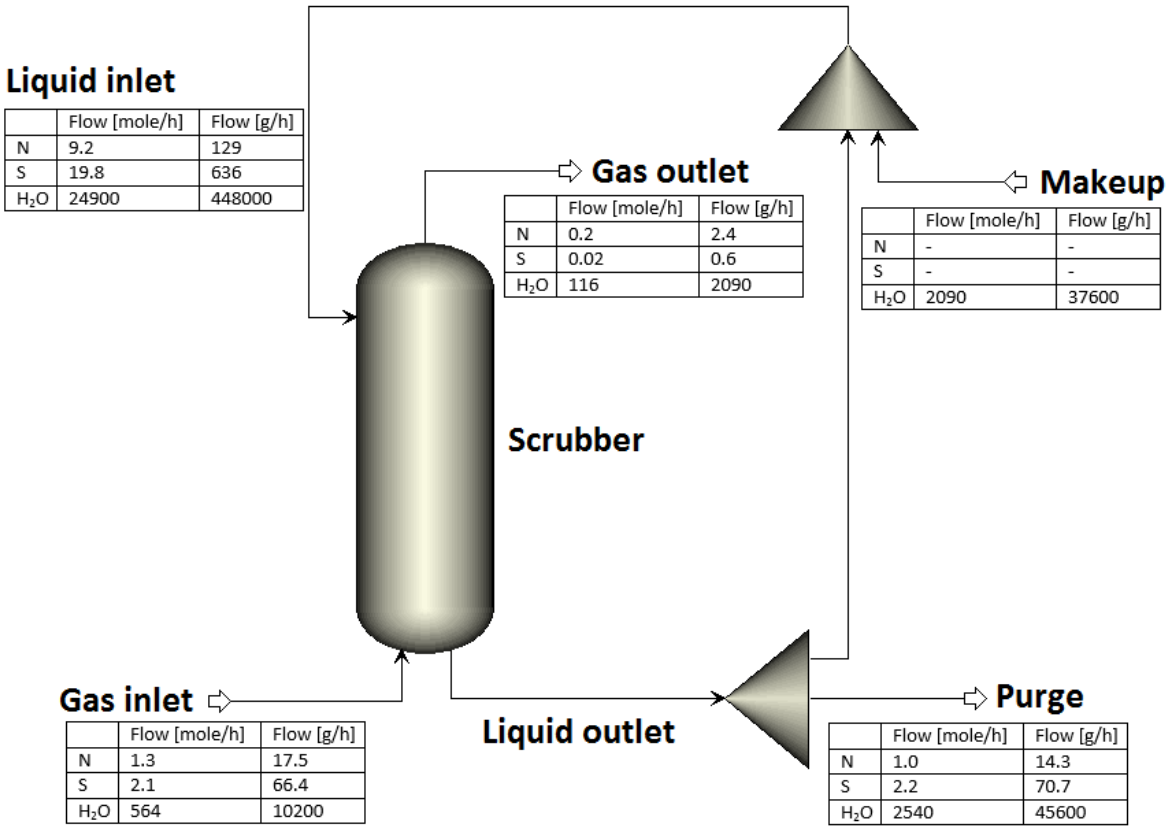

Figure 4.10: Simplified figure of the scrubber with recirculation system from Aspen Plus. Mole- and mass flows are calculated for N, S and H_2O, for a standard case with pH 10 and 5 l/g.

4.3 Recommendations for experimental validation

Table 4.1 shows the cases recommended for experimental validation during the technical scale experiments.

Table 4.1: The table shows the cases recommended for experimental validation during the technical scale experiments.

Case	pH	l/g	SO_2/NO_x [ppm]
1	Self buff.	5-8	500/300
2	4	2.5	500/300
3	10	5-8	500/300
4	10	5-8	750/300

Table 4.2 shows the expected output values for NO_x and SO_2 from the cases recommended for experimental validation in the technical scale experiments in Table 4.1.

Table 4.2: The table shows the expected output values for NO_x and SO_2 from the cases recommended for experimental validation in Table 4.1.

Case	**NO_x gas outlet [ppm]**	**SO_x gas outlet [ppm]**
1	60-65	200-270
2	73	120
3	20-50	1-7
4	70-80	25-50

5
Discussion

5.1 Evaluation of the model

Figure 4.1 shows that approximately all the SO_2 was removed in both cases. The lower section (stage 16-30) of the scrubber removes more SO_2 than the upper section (stage 1-15). The removal was faster for the case with 8 l/g compared to 5 l/g. The reason to the faster removal is because it has more water compared to gas present. The removal in the pure SO_2 cases was as expected [26].

For the case with pure NO_2 in Figure 4.2, 78 % of the NO_2 was removed as nitrite and nitrate were produced. The removal was slightly faster in the lower section of the scrubber, but more constant through the scrubber compared to the removal of SO_2 in Figure 4.1. The pure NO_2 case have a lower removal efficiency of NO_2 than the removal efficiency of SO_2 in the pure SO_2 case. This behavior was expected and is due to the fact that SO_2 has a higher solubility in water compared to NO_2 [26] [27]. The results for the tested case with pure NO is not showed in the results section since nothing happen. NO has low solubility in water and because of that is almost none of the NO absorbed in the scrubber section [28].

For the simultaneous case with both SO_2 and NO_x present, it can be seen in Figure 4.4 that the removal efficiency for NO_x was increased compared to 4.2. The behaviour is expected and is an advantage for the simultaneous removal concept, according to the previous lab-scale experiments made on AkzoNobel. From the evaluation can it be concluded that the results are in accordance with literature which proves that the model can handle the established chemistry well.

5.2 Cases

In Figure 4.3 the case that removed the smallest amount of SO_2 was the self buffering pH with l/g 2.5. All the cases with l/g of 2.5 had the same behavior in the beginning of the lower section (stage 23-30). Further into the scrubber the removal will increase for the 2.5 l/g pH 4-10, but the total removal of SO_2 will not be good enough. The two other self buffering cases with l/g 5 and 8 has a good removal in the lower section, but will stop to remove SO_2 in the upper section of the scrubber. Four models had a similar behavior all through the scrubber and gave a high removal of SO_2, that was with l/g 8 and 5 for pH 10 and 4. The case with 8 l/g and

pH 10 has the fastest removal of SO_2 and results in the lowest amount in the gas outlet. This is because with 8 l/g compared to 5 l/g it will be more water in the system, that will favor the removal of SO_2 according to the literature [26]. A higher pH gives a higher removal efficiency of SO_2 according to the equilibrium reaction 2.3.2. That is the reason why pH 10 gave the highest removal efficiency of SO_2.

In Figure 4.4 more NO_x was removed in the lower section of the scrubber (stage 16-30), compared to the upper section (stage 1-15). The behavior of all cases is similar until the middle of the upper section of the scrubber. The two models that gave the highest removal efficiency are the pH 10 with l/g 8 and 5. The increase in removal that happens in those two models are due to Reaction (2.4.3). That reaction will occur as long as the pH is above or equal to 5 in the scrubber. A higher l/g gave a higher removal of NO_x, as in Figure 4.3. It is because of the same reason that more liquid compared to gas favors the solubility of the NO_x [27].

In Figure 4.5 the removal efficiency of SO_2 are similar for the different pH when l/g is varied. From pH 10 down to pH 4 the difference in removal efficiency is small at a certain l/g, but pH 10 results in the highest removal efficiency. The benefit with pH 4 compared to pH 10 is that lower amounts of NaOH will be needed. A higher l/g also results in a higher removal efficiency. The self buffering case, which results in a pH of about 1.5 has the lowest removal efficiency of all the models. This indicates that the pH should be maintained at higher levels for enhanced performance. The difference in removal efficiency from 5 to 8 l/g for pH 10 down to 4 is small and almost constant, which mean that l/g around 5 and higher give the best removal efficiency of SO_2 and it might not be necessary to have a l/g higher than 5.

In Figure 4.6 the removal efficiency of NO_x is plotted. At low l/g of 2.5 to 4, all models give approximately the same removal efficiency independent of pH. When the l/g is increased, pH 10 results in the highest removal efficiency of NO_x. The relative difference in removal efficiency from 6 to 8 l/g for pH 10 is small, which mean that l/g around 6 and higher give the best removal efficiency of NO_x and it might not be necessary to have a l/g higher than 6.

To see what case that will handle the emission limit corresponding to the BAT in Table 1.1, the results in Figure 4.3-4.6 were studied. From that data, it can be concluded that the cases with pH 10 and 8 to 5 l/g will handle both the SO_2 and NO_x limit. The case with pH 10 and 8 l/g will result in slightly higher removal than the pH 10 and 5 l/g case. The benefits with 5 l/g compared to 8 is that less water is needed with 5 l/g and because of that will smaller equipment and lower amount of chemicals also be needed.

The behavior of the two different l/g cases in Figure 4.7 are similar. Most of the removal of SO_2 and NO_x occurs in the lower section of the scrubber. Compared to Figure 4.3 the removal of SO_2 in this case with 750 ppm happen during a larger part of the scrubber until the removal slows down. In total more SO_2 will be removed since there is more SO_2 present in the scrubber. The removal efficiency of SO_2 will

be decreased compared to the standard case in Figure 4.3. The removal behaviour of NO_x will be similar to the behavior in Figure 4.4, but the removal efficiency of NO_x will be lower. Since more SO_2 is absorbed in the liquid and then more HSO_3^- is produced could that be in favor for the reactions in Table 2.4 and more NO_x should be removed. According to the results in Figure 4.7 will that mechanism not happen and that could be because of the pH in the scrubber will be affected by a higher amount of SO_2 and the pH will be lower inside the scrubber. In Figure 4.4 it could be seen that when the pH was higher or equal to 5 in the scrubber an increase in removal of NO_x was given because of Reaction (2.4.3). In the cases in Figure 4.7 will the pH never be that high inside the scrubber and that will result in a lower removal efficiency of NO_x.

The removal efficiency of SO_2 in Figure 4.8 is close to 100 % for all l/g variations when the case with no sulfite going into the scrubber was simulated. When the sulfite concentration was 3150 mg/l into the scrubber, a higher l/g will give a higher removal efficiency. In Figure 4.8 it can also be seen that the removal efficiency will decrease at a certain l/g when there is a higher concentration of sulfite in the system. The decrease in removal efficiency of SO_2 for the case with 3150 mg/l into the scrubber compared to no sulfite into the scrubber give an expected result, due to the fact that it is more sulfur in the process.

How the removal efficiency of NO_x was affected by the sulfite concentration into the scrubber can be seen in Figure 4.9. The overall behavior of the graph is similar to the one in Figure 4.8, the removal efficiency is lower with a higher concentration of sulfite. That behaviour does not correspond to how it is thought to happen. A higher sulfite concentration should give a higher removal efficiency of NO_x according to the reactions in Table 2.4. The mentioned arguments in the discussion of Figure 4.7 should be valid here too. This mean that the model in Aspen Plus cannot completely describe the complex reaction mechanism in Figure 2.3, due to difficulties in too low pH. To solve the problem with the decreased removal of NO_x at a higher SO_2 concentration the pH needs to be increased inside the scrubber. The concept with increased removal of NO_x with SO_2 present is also discussed during the evaluation. This complex reaction mechanism between NO_x and SO_2 will be interesting to follow up after the technical scale experiments.

The mole- and mass balances in Figure 4.10 are correct for N, S and H_2O. This mean that the model in Aspen Plus can be trusted to solve these calculations and give valid results. The balances over the scrubber occurs in both liquid and gas phase and this mean that the model can handle the equilibrium between absorption and desorption of N and S species. It can be concluded from Figure 4.10 that the reactions inside the scrubber works and produces the correct species. Also that the concerns around the low pH value in the scrubber who causes problems with the reactions between NO_x and SO_2 is not due to errors in the balances.

5.3 Recommendations for experimental validation

The cases recommended for experimental validation in Table 4.1 are selected to give a high variation in ways to operate the scrubber and results received. For case one, there will probably be a lot of SO_2 left in the exhaust gas from the process according to Table 4.2. The predicted results from case three and four are different compared to case one, since most of the SO_2 are expected to be removed in those cases. Case two is predicted to show a removal efficiency of SO_2 between the other cases. Comparing the cases in NO_x removal, the third case is expected to have the lowest amount of NO_x in the gas outlet. The three other cases are predicted to show higher amounts of NO_x and will give similar results to each other. The two most important parameters from the model pH and l/g will be validated in the experiments. Different cases are selected to see how the technical scale experiments will be affected by the variations of the two parameters. The uncertainty about the chemistry when the sulfur concentration are increased in the model discussed in section 5.2 also needs to be experimentally validated. The results from case three and four will be interesting to evaluate to see how the technical scale experiments will handle the chemistry and if it will give a lower output of NO_x in case four compared to three. It would also be interesting to investigate the variation of the pH inside the scrubber, to evaluate the relationship between pH and removed NO_x.

6
Future upscaling

A commercial scale of the discussed process is 10-1000 MW. This section discusses the dimensions and flows that is necessary in the next pilot-plant, which should be around 10 MW.

6.1 Dimensions and flows

To reach 10 MW or more in the process the flow of air and propane needs to be at least 125 times bigger compared to the amount of air and propane used in the 80 kW technical scale experiments. The higher flow of propane and air gives that the exhaust gas into the scrubber are 125 times higher for the 10 MW process. That also mean that the water flow into the scrubber needs to be 125 times bigger, if the same l/g as before shall be reached. In commercial scale of over 10 MW is it more likely that another fuel than propane would be used. Biomass could be an alternative instead of propane, propane have a LHV of 46.3 MJ/kg [25] and biomass have a LHV of about 18.5 MJ/kg [29]. This mean that more than double of the fuel flow would be needed when using biomass and this would also affect the flue gas flow. For simplicity has propane been used as fuel when calculating the dimensions and flows of the scrubber in Figure 6.1.

Renova Sävenäs fourth boiler has a maximum fuel flow of approximately 3.9 kg/s according to [30]. In that plant is waste incinerated, which has the average LHV value of 8.5 MJ/kg [31]. The boiler efficiency is assumed to be 0.9 which gives the maximum boiler capacity of about 30 MW. Which mean a waste fuel flow of about 1.3 kg/s if Renova Sävenäs fourth boiler is recalculated with a capacity of 10 MW. If propane would be used in the upscaled 10 MW case with the LHV value of 46.3 MJ/kg, the propane fuel flow would be 0.22 kg/s. By recalculating this into a fuel flow of biomass and waste would this mean a fuel flow of 0.55 kg/s and 1.2 kg/s respectively. This mean that the upscaled fuel flow originating from the model is of a reasonable size compared to a real case and will be possible to handle in a commercial sized process.

Figure 6.1 shows a simplified figure of the 80 kW and 10 MW scrubbers. The figure shows the dimensions of the scrubbers and the gas flows through them. The counter current liquid is not illustrated in this figure.

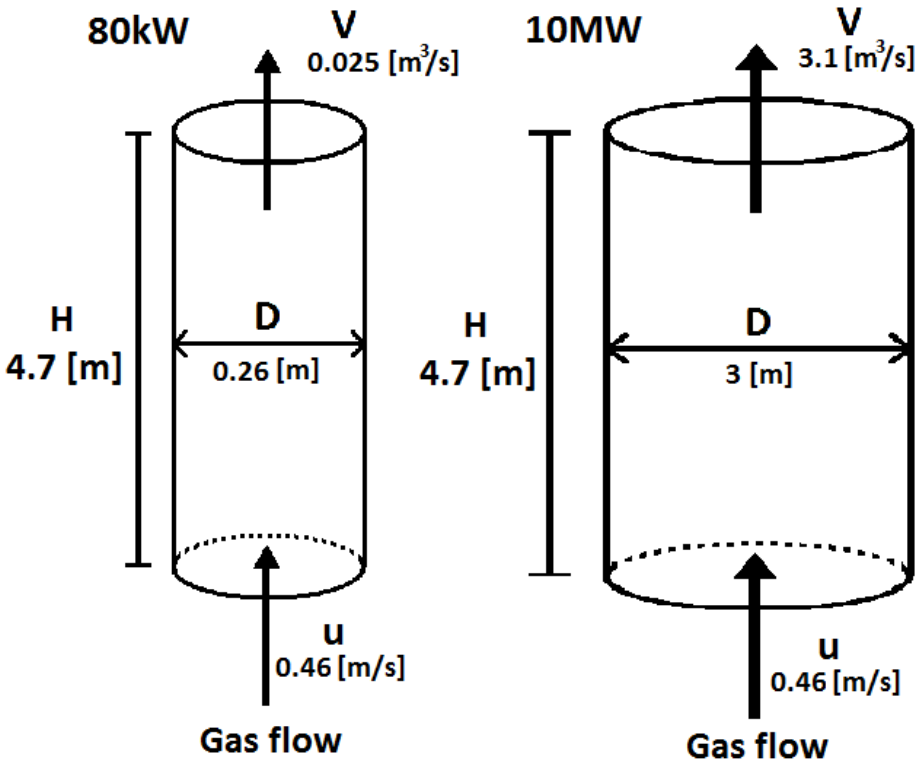

Figure 6.1: Dimensions of the scrubbers and the gas flows through them, pH 10 and 5 l/g. The figure is not in correct scale. The counter current liquid is not illustrated in this figure compared to Figure 2.2.

In Figure 6.1 H is the height of the scrubber [m], D is the diameter [m], u is the gas velocity [m/s] and V is the volume flow [m^3/s].

To calculate the dimensions of the 10 MW scrubber the gas velocity is assumed to be the same through the scrubber as in the 80 kW process, according to Figure 6.1. The height of the scrubber will be constant since the same residence time is enough for the chemistry to occur in the scrubber. The diameter of the 10 MW scrubber is calculated by Equation 6.1 to 3 [m]. In Equation 6.1, u [m/s] is equal to the gas velocity and V [m^3/s] is the up scaled gas volume flow into the scrubber and the values is received from Aspen Plus. All dimensions can be seen in Figure 6.1.

$$u * \pi * \frac{D^2}{4} = V \tag{6.1}$$

Table 6.1 and Table 6.2 shows the flows for ClO_2, NaOH and H_2O in the 80 kW process (from Aspen Plus) and the future upscaled 10 MW process. The values from the 80 kW process are taken from cases with a pH of 10 and 4 in the inlet to the scrubber and a l/g of 5.

Table 6.1: Table of flows of certain chemicals in the 80 kW process with a pH of 10 and l/g of 5 and what to expect of the flows in the 10 MW process.

	ClO_2	NaOH	H_2O
Flows in the 80 kW process [mole/h]	0.61	5.0	2086
Flows in the 80 kW process [g/h]	41.3	200	37500
Flows in the 10 MW process [mole/h]	76.3	625	260000
Flows in the 10 MW process [kg/h]	5.2	25	4690

Table 6.2: Table of flows of certain chemicals in the 80 kW process with a pH of 4 and l/g of 5 and what to expect of the flows in the 10 MW process.

	ClO_2	NaOH	H_2O
Flows in the 80 kW process [mole/h]	0.61	2.38	2089
Flows in the 80 kW process [g/h]	41.3	95.2	37600
Flows in the 10 MW process [mole/h]	76.3	297.5	260000
Flows in the 10 MW process [kg/h]	5.2	11.9	4700

Comparing the flows of the different chemicals in Table 6.1-6.2, the 10 MW needs a higher amount of chemicals. In the case with pH 10, more NaOH will be needed to get that higher pH value into the scrubber compared to the pH 4. The future upscaling needs more investigation and this could be a good starting point for a future master thesis.

To put the amount of chemicals needed in Tables 6.1-6.2 in context it can be compared with the amount of ammonia (NH_3) needed in the SCR method. If the SCR method were used to remove the NO_x instead of the simultaneous removal concept used in this thesis, NH_3 are needed. Approximately all the NO_x will be present as NO after the combustion when SCR are used. The reaction formula for the SCR method are shown in Reaction (7.2).

$$4NO + 4NH_3 + O_2 \rightarrow 4N_2 + 6H_2O \qquad (7.2)$$

Table 6.3 shows the calculated flow of NH_3 if the SCR method would be used to remove NO instead of the simultaneous removal concept described in this thesis. NO and NH_3 are 1:1 in molar ratio, which mean that the amount of removed NO will be the same as the amount of NH_3 used. The removal efficiency of NO_x used, is the same as in the model for pH 10 and l/g 5, 86.5 %.

Table 6.3: Table of flows of NH_3 in a 80 kW and a 10 MW process with a pH of 10 and l/g of 5. The removal efficiency used in this case is the same as in the model for pH 10 and l/g 5, 86.5 %

	NH_3
Flows in 80 kW process [mole/h]	1.08
Flows in 80 kW process [g/h]	33.74
Flows in 10 MW process [mole/h]	134.94
Flows in 10 MW process [kg/h]	4.24

When comparing Table 6.1 and 6.3 it can be seen that approximately the same amount of NH_3 and ClO_2 will be needed. The difference is that with SCR will the removal of NO_x be finished after the SCR, but in the simultaneous removal concept in this thesis will the flue gases also be scrubbed before the removal is finished. That is why H_2O and NaOH is needed and therefore more chemicals, but instead will also SO_2 be removed. Removal efficiency for NO_x by SCR is 80-90 %, but the simultaneous concept described in this thesis can achieve a higher removal efficiency. In Appendix A.2 the removal efficiency for NO_x with pH 10 l/g 8 in Table A.2 can be seen, 92.9 %. Further investigation of the amount of chemicals is needed, that includes economical and environmental comparison for example.

7
Conclusion

A model has been created in Aspen Plus to simulate the technical scale experiments. The model is used to identify the important process parameters and to give recommendations for experimental validation. The evaluation of the model showed results that are in accordance with literature. That mean that the model can handle the established chemistry well as long as the ppm value of SO_2 in the gas inlet to the scrubber is below 500. From the results of the simulated cases it was found that pH 10 in the liquid into the scrubber was the alternative that gave the highest removal of both SO_2 and NO_x. According to the emission limits from BAT in Table 1.1 the case with a l/g of 8 and pH 10 in Table A.2 gave the highest removal, the gas outlet contained 21 ppm NO_x and 1 ppm SO_2. A lower l/g in form of 5 and a pH of 10 will require a lower amount of chemicals and smaller equipment sizes and will still be enough to meet the BAT emission limits, the gas outlet contained 44 ppm NO_x and 7 ppm SO_2.

To the technical scale experiments that will be performed in the Chalmers 100 kW oxy-fuel unit, a pH of 10 and l/g of 5 to 8 is expected to be the process parameters that will give the highest removal. A recommendation for experimental validation of the model during the technical scale experiments is created and it shows four cases with large variation in the expected results. The results from the simulated case with higher sulfite concentration into the scrubber in Figure 4.9 showed that the model did not completely follow the reaction mechanisms in Figure 2.3, since the pH will be too low in the scrubber. This pH dependent chemistry needs further investigation and is important to test during the technical scale experiments. Upscaling the concept to commercial scale of over 10 MW will give larger flows and diameter of the scrubber. The upscaled flows and dimensions seemed reasonable, but this upscaling needs further investigation. By combining the results from the simulations in Aspen Plus done in this thesis, the discussion in Chapter 6 and the results from the technical scale experiments another master thesis on this concept can be done.

8
Future work

Important areas for future work identified during this master thesis includes the reaction mechanism in the scrubber, the pH inside the scrubber and upscaling of this process.

The reaction mechanism and especially the pH dependent reactions in Table 2.4 need to be further developed. Especially, the effect on the reaction mechanism from increased sulfite concentration in the liquid inlet to the scrubber needs to be further developed and investigated, due to the results in Figure 4.9. The pH profile inside the scrubber need more investigation since the pH inside the scrubber during the simulations gets to low and will not favour the removal of NO_x.

When comparing the results from the Aspen Plus simulations with the technical scale experiments, the results could differ due to the time aspect. Aspen Plus will give results from simulations with steady state but the technical scale experiments will probably never reach steady state and always be in dynamic mode. An evaluation of this time perspective would be interesting and to see the effect of it.

Another interesting subject to look into in a future master thesis is the upscaling from 80 kW to commercial scale of over 10 MW. By combining the results from the simulations in Aspen Plus done in this thesis, the discussion in Chapter 6 and the results from the technical scale experiments another master thesis on this process could be done.

Bibliography

[1] European Union, *Directive 2010/75/EU of the European Parliament and of the Council on industrial emissions*, Official Journal of the European Union, 2010, pp. 59 – 61.

[2] Haunstetter, J., & Weinhart, N. (2015). Evaluation of a Novel Concept for Combined NOx and SOx Removal. Göteborg: Chalmers University of Technology.

[3] Ajdari, S., Normann, F., Andersson, K., & Johnsson, F. (2016). Reduced Mechanism for Nitrogen and Sulfur Chemistry in Pressurized Flue Gas Systems. Gothenburg: American Chemical Society.

[4] Ajdari, S., Normann, F., Andersson, K., & Johnsson, F. (2014). Modeling the Nitrogen and Sulfur Chemistry in Pressurized Flue Gas. Gothenburg: American Chemical Society.

[5] Ibrahim, S. (2016). Process evaluation of a SOx and NOx exhaust gas cleaning concept for marine application. Gothenburg: Chalmers University of Technology.

[6] Richards, J. R. (2000). Control of Nitrogen Oxides Emissions. United States: ICES Ltd. pp. 10-16 - 10-19, 2-4 - 2-10, 12-3 - 12-7, 7-3 - 7-4.

[7] Krawczyk, E., Zajemska, M., & Wylecial, T. (2013). The chemical mechanism of SOx formation and elimination in coal combustion processes. CHEMIK, pp. 856-862.

[8] Comission on natural resources, National academy of sciences, National academy of engineering & National Research council. (1975). Air quality and stationary source emission control. Washington: U.S Government printing office.

[9] Arthur L Kohl, a. R. (1997). Gas Purifaction. Houston: Elsevier Science. pp. 496-500, 539-544.

[10] Brogren, C., & Karlsson, H. T. (1997). Modeling the absorption of SO2 in a spray scrubber using the penetration theory. Västerås: Elsevier. 52(18), 3085-3099.

[11] Athir, 2018. Two Film Theory. [Online] Available at: https://www.scribd.com/document/223397581/Two-Film-Theory [Used 11 03 2018].

[12] Yamuni, K. (2018, Januari 18). Chemistry Libretexts. Retrieved from https://chem.libretexts.org/Core/Physical_and_Theoretical_Chemistry/Physical_Properties_of_Matter/Solutions_and_Mixtures/Ideal_Solutions/Dissolving_Gases_In_Liquids%2C_Henry's_Law.

[13] Atkinson, R., Baulch, D. L., Cox, R. A., Crowley, J. N., Hampson, R. F., Hynes, R. G., . . . Troe, J. (2005). Evaluated kinetic and photochemical data for atmospheric chemistry: Volume III – gas phase reactions of inorganic halo-

gens. Atmospheric Chemistry and Physics: Copernicus GmbH on behalf of the European Geosciences Union.

[14] Eibling, R. E., & Kaufman, M. (1982). Kinetics studies relevant to possible coupling between the stratospheric chlorine and sulfur cycles. Atlanta: Department of Chemistry, Emory University.

[15] Watson, R. T. (1977). Rate constants for reactions of ClOx of atmospheric interest. California: American Institute of Physics. pp. 888.

[16] Watson, R. T. (1977). Rate constants for reactions of ClOx of atmospheric interest. California: American Institute of Physics.

[17] Lee, Y. -N., & Schwartz, S. (1981). Reaction Kinetics of Nitrogen Dioxide with Liquid Water at Low Partial Pressure. New York: Environmental Chemistry Division, Department of Energy and Environment, Brookhaven National Laboratory, Upton. pp. 840-848.

[18] Park, J.-Y., & Lee, Y.-N. (1988). Solubility and Decomposition Kinetics of Nitrous in Aqueous solution. New York: Environmental Chemistry Division, Department of Applied Science, Brookhaven National Laboraty.

[19] Atkinson, R., Baulch, D., Cox, R., Crowley, J., Hampson, R., Hynes, R., . . . Troe, J. (2003). Evaluated kinetic and photochemical data for atmospheric chemistry: Volume 1 - gas phase reactions of Ox, HOx, NOx and SOx species. Atmospheric Chemistry and Physics.

[20] Niu, Z., Guo, Y., Zeng, Q., & Lin, W. (2012). Experimental studies and Rate-Based process Simulations of CO2 Absorption with Aqueous Ammonia Solutions. 5309-5319.

[21] Siddiqi, M. A., Krissmann, J., Peters-Gerth, P., Luckas, M., & Lucas, K. (1996). Spectrophotometric measurement of the vapour-liquid equilibria of (sulphur dioxide + water). J. Chem. Thermodynamics, 28, 685-700.

[22] Beilke, S., & Gravenhorst, G. (1978). Heterogeneous SO2-oxidation in the droplet phase. Atmos. Environ., 12, 231-239.

[23] Oblath, S. B., Markowitz, S. S., Novakov, T., & Chang, S. G. (1982). Kinetics of the formation of the initial reaction of nitrite ion in bisulfite solutions. J. Phys. Chem., 86, 4853-4857.

[24] Clifton, C. L., Alstein, N., & Huie, R. E. (1988). Rate-constant for the reaction of NO2 with sulfur(IV) over the pH range 5.3-13. Environ. Sci. Technol., 22, 586-589.

[25] Boundy, B., Diegel, S., Wright, L., & Davis, S. (2011). Biomass Energy ata Book: Edition 4. Tennessee: U.S DEPARTMENT OF ENERGY.

[26] TOXNET. (2018, 05 29). HSDB: Sulfur dioxide. Retrieved from NIH U.S. National Library of Medicine: https://toxnet.nlm.nih.gov/cgi-bin/sis/search2/r?dbs+hsdb:@term+@rn+@rel+7446-09-5

[27] (BMZ), G. F. (1994). Volume III: Compendium of environmental standards. Berlin: Ó Deutsche Gesellschaft für Technische Zusammenarbeit (GTZ) GmbH.

[28] TOXNET. (2018, 05 29). HSDB: Nitrogen monoxide. Retrieved from NIH U.S. National Library of Medicine: https://toxnet.nlm.nih.gov/cgi-bin/sis/search2/r?dbs+hsdb:@term+@rn+@rel+7446-09-5

[29] Zhang, Y., Gao, X., Li, B., Zhang, H., Qi, B., Wu, Y. (2015). An expeditious methodology for estimating the exergy of woody biomass by means of heating values. 712-719.
[30] Egle, A. (2007, 08 29). Renova investerar 600 miljoner i fjärde panna i Sävenäs.
[31] Maria, F. D., Lasagni, M. (2017). On line measurement of the lower heating value of waste and energetic efficiency of an existing waste to energy plant: Identification of uncertainty associated to probes and their influence on the results. Lecce: Elsevier.

A

Appendix

A.1 Pictures of the process from the technical scale experiments

Pictures of the 100 kW oxy-fuel unit at Chalmers will be shown in this appendix. In this process will the technical scale experiments be performed and it is for this process that the experimental plan and process parameters has been recommended. These pictures can be compared with the simple process overview in Figure 2.1, to get an understanding of how the process looks like in reality. They can also be compared with Figure 3.1 that shows how the process was modeled in Aspen Plus.

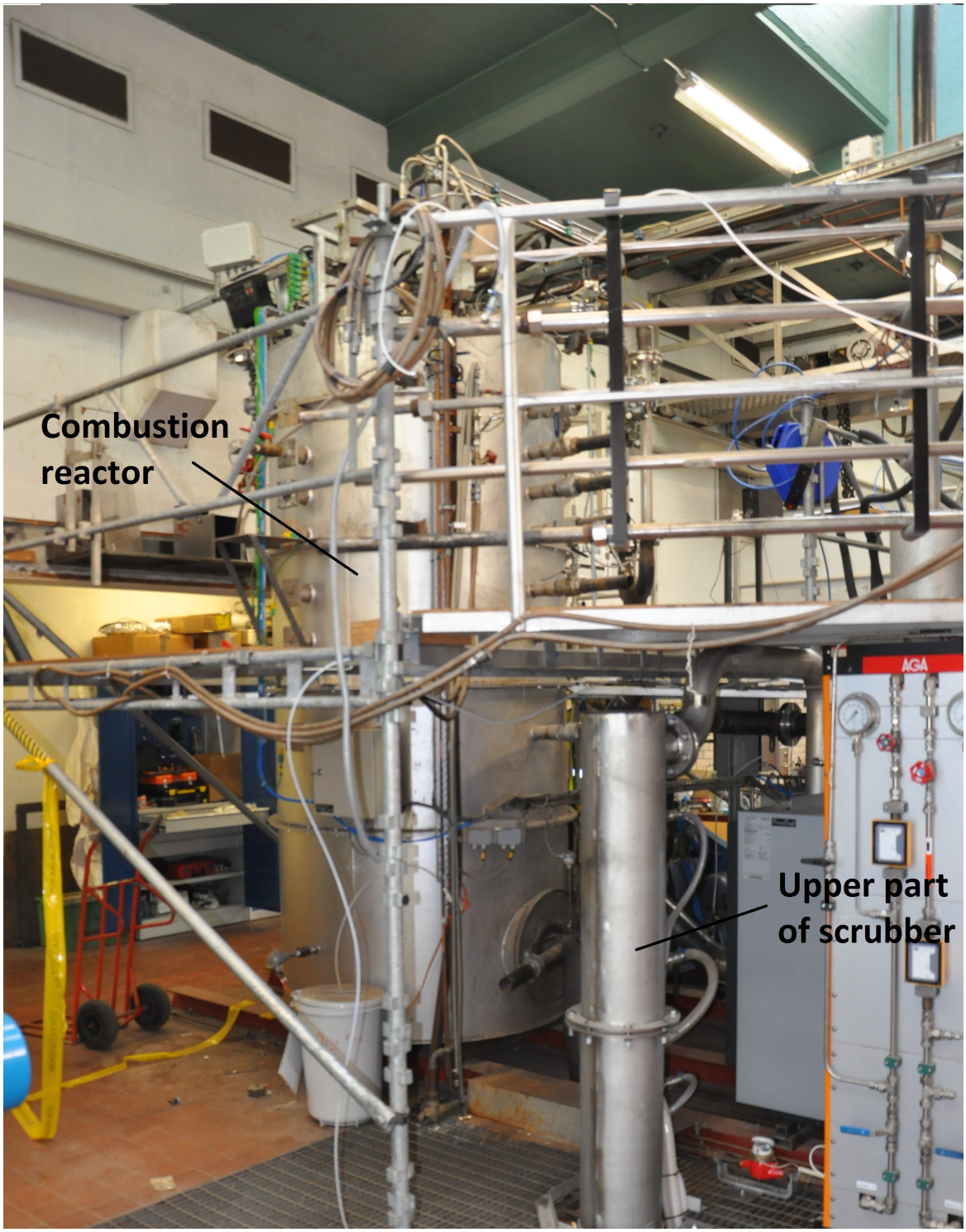

Figure A.1: Picture of the combustion reactor used in the technical scale experiments at Chalmers 100kW oxy-fuel unit.

Figure A.2: Picture of the cooler located after the combustion reactor in Figure 2.1, the one used in the technical scale experiments at Chalmers 100kW oxy-fuel unit.

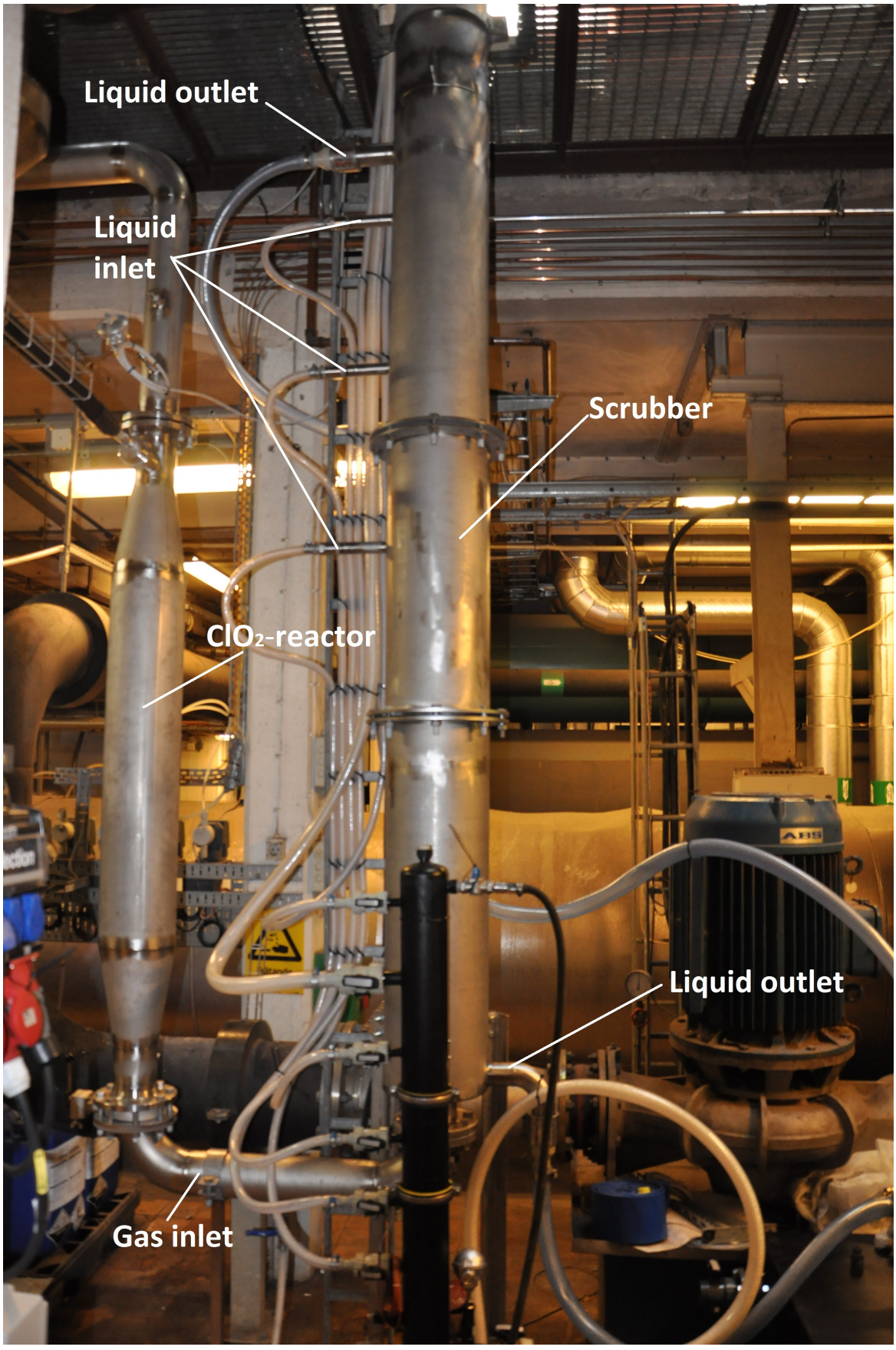

Figure A.3: Picture of the scrubber used in the technical scale experiments at Chalmers 100kW oxy-fuel unit, this picture can be compared with Figure 3.2.
IV

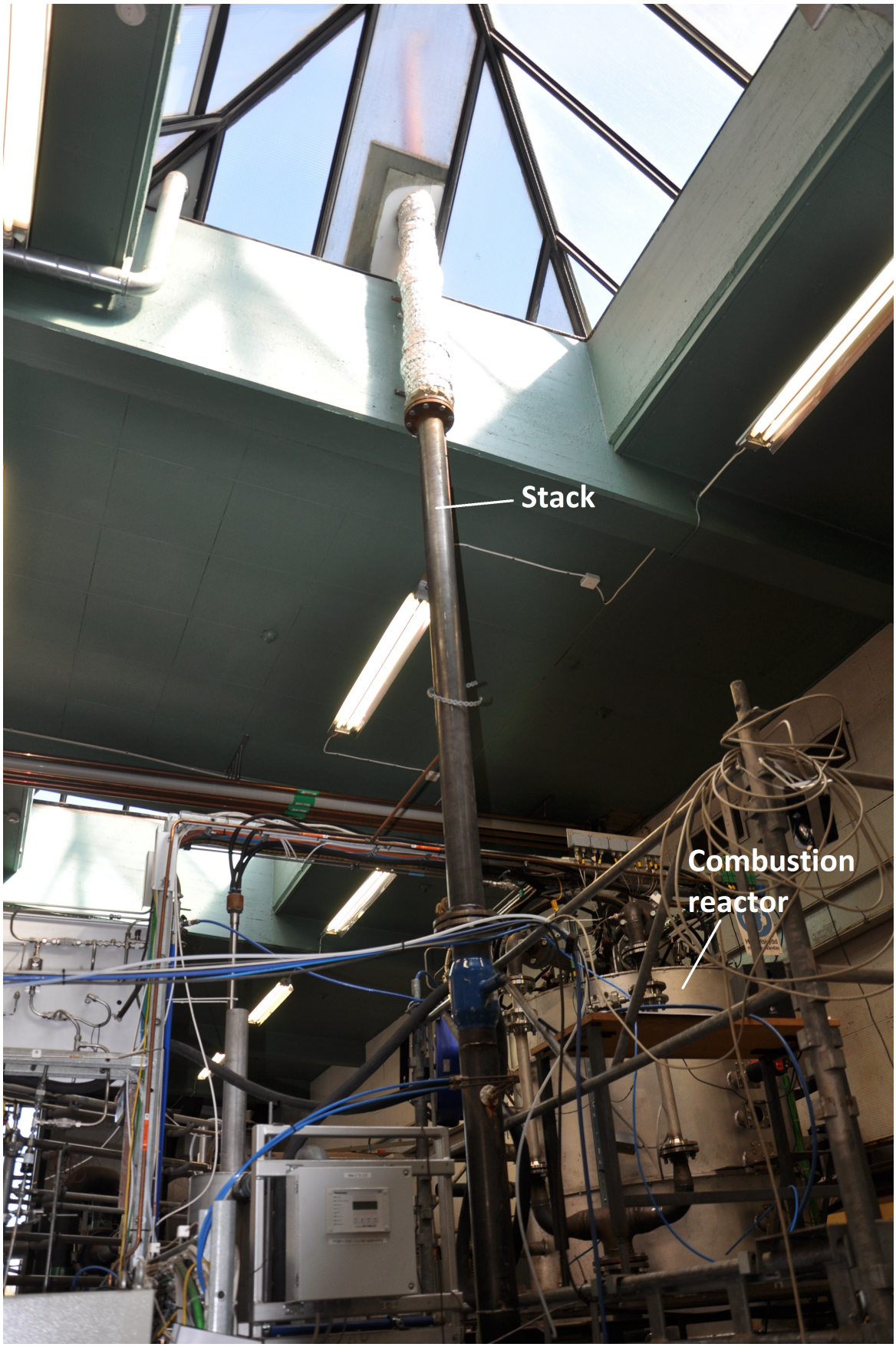

Figure A.4: Picture of the stack that releases the cleaner flue gases after the scrubber, from the technical scale experiments at Chalmers 100kW oxy-fuel unit.

A.2 Tables from the results

Table A.1: The results from the model evaluation with pure SO_2, NO_2 and NO. The pH was 10 in the inlet to the scrubber. The standard amount of SO_2 and NO_x was used in the inlet to the scrubber which are 500 ppm and 300 ppm.

Parameter	**8 l/g SO_2**	**5 l/g SO_2**	**8 l/g NO_2**	**8 l/g NO**
Removal efficiency SO_2 (%)	100	99.3	-	-
Removal efficiency NO_x (%)	-	-	78	0
Gas outlet SO_2 (ppm)	0.14	4.2	-	-
Gas outlet NO_2 (ppm)	-	-	73	-
Gas outlet NO (ppm)	-	-	0.97	338
Liquid outlet $C_{NO_2^-}$ (mg/l)	-	-	310	0
Liquid outlet $C_{NO_3^-}$ (mg/l)	-	-	420	0
Liquid outlet $C_{SO_3^{2-}}$ (mg/l)	2320	3600	-	-
Liquid outlet $C_{SO_4^{2-}}$ (mg/l)	0	0	-	-
pH outlet	2.4	2.26	3.86	10

Table A.2: The results from three cases with pH 10 in the inlet to the scrubber and l/g of; 8, 5 and 2.5. The standard amounts of SO_2 and NO_x was used in the inlet to the scrubber, which are 500 ppm and 300 ppm respectively.

Parameter	**8 l/g**	**5 l/g**	**2.5 l/g**
Removal efficiency SO_2 (%)	99.8	98.7	79.8
Removal efficiency NO_x (%)	92.9	86.5	77.1
Gas outlet SO_2 (ppm)	1	7.1	113
Gas outlet NO_2 (ppm)	21	44	77
Gas outlet NO (ppm)	3	2	0.14
Gas outlet N_2O (ppm)	18	17	24
Liquid outlet $C_{NO_2^-}$ (mg/l)	120	40	14
Liquid outlet $C_{NO_3^-}$ (mg/l)	410	680	1430
Liquid outlet $C_{NO_2^-}/C_{NO_3^-}$ (mol/mol)	0.39	0.075	0.014
Liquid outlet $C_{SO_3^{2-}}$ (mg/l)	1120	2160	3360
Liquid outlet $C_{SO_4^{2-}}$ (mg/l)	380	360	790
Liquid outlet $C_{SO_3^{2-}}/C_{SO_4^{2-}}$ (mol/mol)	3.5	7.2	5.17
Liquid outlet HADS (mg/l)	1150	1720	2480
pH outlet	2.5	2.2	2.1

Table A.3: The results from three cases with pH 4 in the inlet to the scrubber and l/g of; 8, 5 and 2.5. The standard amounts of SO_2 and NO_x was used in the inlet to the scrubber, which are 500 ppm and 300 ppm respectively.

Parameter	**8 l/g**	**5 l/g**	**2.5 l/g**
Removal efficiency SO_2 (%)	99.1	97.9	78.6
Removal efficiency NO_x (%)	79.1	78.8	78.5
Gas outlet SO_2 (ppm)	4.5	11.8	119.8
Gas outlet NO_2 (ppm)	70	71.4	72.7
Gas outlet NO (ppm)	0.45	0.26	0.21
Gas outlet N_2O (ppm)	12	18	18
Liquid outlet $C_{NO_2^-}$ (mg/l)	34	22	17
Liquid outlet $C_{NO_3^-}$ (mg/l)	500	740	1550
Liquid outlet $C_{NO_2^-}/C_{NO_3^-}$ (mol/mol)	0.093	0.04	0.014
Liquid outlet $C_{SO_3^{2-}}$ (mg/l)	1520	2240	2960
Liquid outlet $C_{SO_4^{2-}}$ (mg/l)	140	310	600
Liquid outlet $C_{SO_3^{2-}}/C_{SO_4^{2-}}$ (mol/mol)	13	8.5	5.9
Liquid outlet HADS (mg/l)	920	570	690
pH outlet	2.3	2.13	2.07

Table A.4: The results from three cases with self buffering pH in the inlet to the scrubber and the l/g of; 8, 5 and 2.5. The standard amounts of SO_2 and NO_x was used in the inlet to the scrubber, which are 500 ppm and 300 ppm respectively.

Parameter	**8 l/g**	**5 l/g**	**2.5 l/g**
Removal efficiency SO_2 (%)	64.14	52.6	26.18
Removal efficiency NO_x (%)	81.47	81.48	77.63
Gas outlet SO_2 (ppm)	206.2	265.4	412.5
Gas outlet NO_2 (ppm)	63.2	61.0	62.2
Gas outlet NO (ppm)	1.3	1.67	13.5
Gas outlet N_2O (ppm)	22.6	23.4	51.5
Liquid outlet $C_{NO_2^-}$ (mg/l)	30	40	110
Liquid outlet $C_{NO_3^-}$ (mg/l)	520	870	1360
Liquid outlet $C_{NO_2^-}/C_{NO_3^-}$ (mol/mol)	0.086	0.061	0.103
Liquid outlet $C_{SO_3^{2-}}$ (mg/l)	400	370	210
Liquid outlet $C_{SO_4^{2-}}$ (mg/l)	120	360	1540
Liquid outlet $C_{SO_3^{2-}}/C_{SO_4^{2-}}$ (mol/mol)	3.96	1.24	0.16
Liquid outlet HADS (mg/l)	380	500	-
pH inlet	1.76	1.65	1.42
pH outlet	1.68	1.57	1.396

Table A.5: The results from non-standard S/NO_x cases with 750ppm SO_2 and 300ppm NO_2 in the gas inlet to the scrubber. The pH values of 10 and 4 was used in the inlet to the scrubber in the two different simulations and l/g of 5 was used in both.

Parameter	**5 l/g**	**5 l/g**
Removal efficiency SO_2 (%)	96.7	93.7
Removal efficiency NO_x (%)	77.2	78.3
Gas outlet SO_2 (ppm)	27	49
Gas outlet NO_2 (ppm)	77	73
Gas outlet NO (ppm)	0.083	0.085
Gas outlet N_2O (ppm)	21	21.5
Liquid outlet $C_{NO_2^-}$ (mg/l)	10	10
Liquid outlet $C_{NO_3^-}$ (mg/l)	680	740
Liquid outlet $C_{NO_2^-}/C_{NO_3^-}$ (mol/mol)	0.02	0.018
Liquid outlet $C_{SO_3^{2-}}$ (mg/l)	4000	3680
Liquid outlet $C_{SO_4^{2-}}$ (mg/l)	340	380
Liquid outlet $C_{SO_3^{2-}}/C_{SO_4^{2-}}$ (mol/mol)	14.7	12.1
Liquid outlet HADS (mg/l)	1340	1340
pH inlet	10	4
pH outlet	2.1	2.06